

NASA CR-121198
WANL-M-FR-72-011

NASA-CR-121198) STUDY OF GAS TUNGSTEN
ARC WELDING PROCEDURES FOR TANTALUM ALLOY
T-111 (Ta-8 W-2Hf) PLATE Final Report,
1971 - (Westinghouse Astronuclear Lab.,
Pittsburgh) 93 p HC \$6.50

N73-28530

Unclas
10046

G3/15

CSCL 13H

**STUDY OF GAS TUNGSTEN-ARC
WELDING PROCEDURES
FOR
TANTALUM ALLOY T-111 (Ta-8W-2Hf) PLATE**

BY

R. E. GOLD AND L. KESTERSON

WESTINGHOUSE ASTRONUCLEAR LABORATORY

MAY, 1973

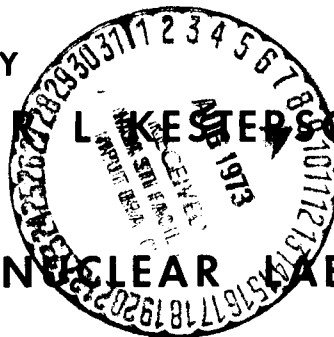
CONTRACT NAS 3-15555

prepared for

NATIONAL AERONAUTICS AND SPACE ADMINISTRATION

NASA LEWIS RESEARCH CENTER
CLEVELAND, OHIO

THOMAS J. MOORE, PROJECT MANAGER
MATERIALS AND STRUCTURES DIVISION



NOTICE

This report was prepared as an account of Government-sponsored work. Neither the United States, nor the National Aeronautics and Space Administration (NASA), nor any person acting on behalf of NASA:

- A.) Makes any warranty or representation, expressed or implied, with respect to the accuracy, completeness, or usefulness of the information contained in this report, or that the use of any information, apparatus, method, or process disclosed in this report may not infringe privately-owned rights; or
- B.) Assumes any liabilities with respect to the use of, or for damages resulting from the use of, any information, apparatus, method or process disclosed in this report.

As used above, "person acting on behalf of NASA" includes any employee or contractor of NASA, or employee of such contractor, to the extent that such employee or contractor of NASA or employee of such contractor prepares, disseminates, or provides access to any information pursuant to his employment or contract with NASA, or his employment with such contractor.

Requests for copies of this report should be referred to

National Aeronautics and Space Administration
Scientific and Technical Information Facility
P. O. Box 33
College Park, Maryland 20740

1. Report No. NASA CR-121198	2. Government Accession No.	3. Recipient's Catalog No.	
4. Title and Subtitle Study of Gas Tungsten-Arc Welding Procedures for Tantalum Alloy T-111 (Ta-8W-2Hf) Plate		5. Report Date May, 1973	6. Performing Organization Code
		8. Performing Organization Report No. WANL-M-FR-72-011	
7. Author(s) R. E. Gold and R. L. Kesterson		10. Work Unit No.	
9. Performing Organization Name and Address Westinghouse Astronuclear Laboratory P. O. Box 10864 Pittsburgh, Pennsylvania 15236		11. Contract or Grant No. NAS 3-15555	
		13. Type of Report and Period Covered Final Report 1971-1972	
12. Sponsoring Agency Name and Address National Aeronautics and Space Administration Washington, D. C. 20546		14. Sponsoring Agency Code	
		15. Supplementary Notes Thomas J. Moore , Project Manager, Materials and Structures Division, NASA Lewis Research Center, Cleveland, Ohio	
16. Abstract <p>Methods of eliminating or reducing underbead cracking in multipass GTA welds in thick T-111 plate were studied. Single "V" butt welds prepared using experimental filler metal compositions and standard weld procedures resulted in only moderate success in reducing underbead cracking. Subsequent procedural changes incorporating manual welding, slower weld speeds, and three or fewer fill passes resulted in crack-free single "V" welds only when the filler metal was free of hafnium. The double "V" joint design with successive fill passes on opposite sides of the joint produced excellent welds.</p> <p>The quality of each weld was determined metallographically since the cracking, when present, was very slight and undetectable using standard NDT techniques. Tensile and bend tests were performed on selected weldments. The inherent filler metal strength and the joint geometry determined the strength of the weldment .</p> <p>Hardness and electron beam microprobe traverses were made on selected specimens with the result that significant filler metal-base metal dilution as well as hafnium segregation was detected. A tentative explanation of T-111 plate underbead cracking is presented based on the intrinsic effects of hafnium in the weldment.</p>			
17. Key Words (Suggested by Author(s)) Welding - Gas Tungsten Arc Tantalum Alloys - T-111 Refractory Metal Fabrication		18. Distribution Statement Unclassified - Unlimited	
19. Security Classif. (of this report) Unclassified	20. Security Classif. (of this page) Unclassified	21. No. of Pages 85	22. Price*

* For sale by the National Technical Information Service, Springfield, Virginia 22151

FOREWORD

The work described in this report was carried out by personnel of the Westinghouse Astronuclear Laboratory under Contract NAS 3-15555 for the NASA-Lewis Research Center. The work was administered at the Astronuclear Laboratory by Messrs. R. W. Buckman, Jr. and L. G. Stemann, Jr. Mr. T. J. Moore was the NASA Project Manager for this program.

Primary units in this report are the International System of Units (or System Internationale d'Unites, Reference NASA SP-7012). For clarity, the customary engineering units have also been provided as secondary units. All measurements made in the experimental work utilized the latter units.

TABLE OF CONTENTS

	<u>Page No.</u>	
1.0	SUMMARY	1
2.0	INTRODUCTION	3
3.0	PROGRAM AND PROCEDURES	5
	3.1 Technical Program	5
	3.2 Program Materials	7
	3.3 Filler Metal Composition Selection	13
	3.4 Varestraint Testing	16
	3.5 Butt Welding Evaluation	19
	3.5.1 Initial Series (Welds 1-13; Single "V" Configuration)	19
	3.5.2 Second Series (Welds 14-29; Varied Configurations)	23
4.0	RESULTS AND DISCUSSION	29
	4.1 Filler Metal Characterization	29
	4.2 Varestraint Results	35
	4.3 Plate Weldment Studies	43
	4.4 Procedural and Design Changes	51
	4.5 Tensile Tests	61
	4.6 Bend Tests	64
	4.7 Microprobe Analysis	68
	4.8 Hardness Tests	74
5.0	CONCLUSIONS	78
6.0	REFERENCES	79

LIST OF ILLUSTRATIONS

<u>Figure No.</u>	<u>Title</u>	<u>Page No.</u>
1	Program Outline	6
2	As-cast Buttons of Filler Metals 1 through 8	9
3	Location of Nominal Filler Metal Compositions on the Ta-W-Hf Ternary Phase Diagram	15
4	Varestraint Test Apparatus	17
5	Schematic: Bending Technique for Augmenting Strain by Varestraint Testing	18
6	Preparation and Test Concept for Varestraint Evaluation of Filler Wire	20
7	Configuration Used for Single "V" Plate Welds	22
8	Configuration Used for (Modified) Single "U" Plate Welds	24
9	Configuration Used for Double "V" Plate Welds	25
10	Schematic: Orientation of Tensile Specimens Within Plate Welds	27
11	As-cast Microstructures - FM 3 and 6	30
12	As-cast Microstructures - FM 7 and 8	31
13	Typical Rolled/Annealed Microstructures - FM 4 and 8	32
14	As-polished Varestraint Crack Patterns in FM 1 and FM 6	36
15	As-polished Varestraint Crack Patterns in FM 7 and FM 8	37
16	Microstructures of Single "V" Welds 2 and 4	46
17	Microstructures of Single "V" Welds 6 and 8	47
18	Microstructures of Single "V" Welds 9 and 10	48
19	Microstructures of Single "V" Welds 11 and 12	49
20	Microstructure of Single "V" Weld 13	50
21	Example of Grain Boundary Sliding in Multipass GTA Plate Weldment	52
22	Example of Grain Boundary Cracking in Multipass GTA Plate Weldment	53
23	Microstructure of Single "V" Weld 14	55
24	Microstructure of Single "V" Weld 18	56

LIST OF ILLUSTRATIONS (Cont'd.)

<u>Figure No.</u>	<u>Title</u>	<u>Page No.</u>
25	Microstructure of Double "V" Weld 20	58
26	Microstructure of Double "V" Weld 22	59
27	Microstructure of Double "V" Weld 29	60
28	As-tested Tensile Specimens. Specimens Machined from Multipass GTA Plate Weldments.	63
29	Relationship Between Filler Metal Hardness and Weld Strength at Ambient Temperature	65
30	Typical Results of Dye Penetrant Inspection of As-Welded Butt Welds	66
31	As-Bend Tested Plate Weld Specimen. Single "V" Weld Tested with Top Face of Weldment in Tension.	69
32	As-Bend Tested Plate Weld Specimen. Single "V" Weld Tested with Top Face of Weldment in Tension.	70
33	Microstructure of Single "V" Weld 19 - Before and After Bend Testing	71
34	Microstructure of Single "U" Weld 24 - Before and After Bend Testing	72
35	Typical Microstructure of Double "V" Weld 23 Following Bend Test at Room Temperature	73
36	Schematic: Location of Hardness Measurements on Plate Weldments. Data Tabulated on Table 12	76

LIST OF TABLES

<u>Table No.</u>	<u>Title</u>	<u>Page No.</u>
1	As-Received Chemical Analyses of Starting Material	8
2	Chemical Analyses of Filler Metal Compositions	11
3	Chemical Analyses of Production Filler Metal Compositions	12
4	Nominal Filler Metal Compositions	14
5	Results of Hardness Measurements on Filler Metal Compositions	34
6	Varestraint Crack Count Data	39
7	Summary of Varestraint Data	40
8	Ranking of Filler Metals According to Results of Varestraint Tests	42
9	Plate Weldment Records	44
10	Tensile Test Results	62
11	Results of Bend Tests on Welded Joints	67
12	Weldment Hardness Results	75

1.0 SUMMARY

The effects of filler metal compositions, welding procedures, and joint geometry on underbead cracking of multipass gas tungsten-arc (GTA) welds on 0.952 cm (.375 in.) thick T-111 (Ta-8W-2Hf) plate were studied. This investigation was prompted by previous observations of a propensity for underbead cracking in thick T-111 plate GTA welded with T-111 filler wire. Thirteen filler metal compositions spanning the tantalum-rich portion of the Ta-W-Hf ternary phase diagram were studied. The Varestraint test was used early in the program to screen eight of the filler metal compositions for hot cracking tendencies.

Following the initial screening studies the four most promising alloys and a series of "base-line" filler metals were used for plate weld tests using a single "V" groove weld in T-111 plate. Each of the initial series of butt welds were made using standard multipass GTA weld techniques. The presence and extent of underbead cracking was determined by metallographic examination. Evaluation of these welds indicated only modest improvements could be realized by attempts to metallurgically remedy the problem with filler metal composition variations.

A modified welding procedure incorporating manual welding, low welding speeds, and a limited number of passes (3 or less) was developed which produced crack-free welds in single "V" joints of T-111 plate but only with hafnium-free filler metals. When this procedure was applied to hafnium-containing filler metals, cracking occurred but on a reduced scale. Two of the better performing filler metals, Ta-4W-1Hf and Ta-4W, were chosen for use in further weld procedural and joint design studies. Wire of each of these compositions was produced from a consumable electrode melted ingot by a combination of hot extrusion and cold swaging.

Alternate joint designs including the double "V" and single "U" were studied. The single "U" joint was designed to reduce the amount of filler metal required per joint and thus limit heat input and thermal cycling. This approach did not provide significant improvement.

The double "V" design, because of the inherent balancing of stresses as successive weld beads are placed on opposite sides, resulted in sound weld structures. It is recognized that the use of this joint design is severely limited in practice because of the necessity for access to both sides of the weld joint.

Specimens removed from selected weldments were tensile tested at room temperature and 1649°C (3000°F) and tested in bending at room temperature. With severe (90°) bends around a 1 t radius, cracking was evident, but the cracks did not propagate catastrophically.

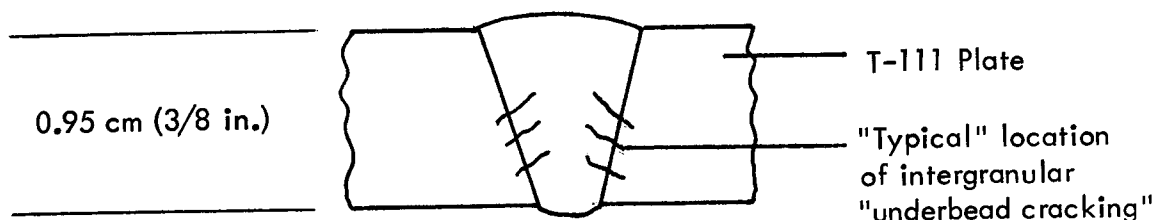
Hardness traverses and electron microprobe analyses indicated a substantial effect of base-metal dilution throughout the weldment. Hafnium segregation was observed in the weld metal, at grain boundaries, and along solute lines. The presence of hafnium in the highly stressed grain boundary areas appears to be a very important factor contributing to the under-bead cracking in single "V" T-111 GTA plate welds.

2.0 INTRODUCTION

Previous results of welding research with T-111 (Ta-8W-2Hf) plate^(1,2,3) have demonstrated this alloy to be sensitive to "underbead cracking"* in multipass gas tungsten-arc (GTA) weldments. This cracking occurs in the initial passes of manual GTA plate welds during subsequent deposition of intermediate and final passes. The cracks invariably occur at grain boundaries and frequently extend into the heat affected zone (HAZ). In T-111 this problem is only encountered in plate of section thicknesses greater than approximately 0.95 cm (3/8 in.).

The basic mode of underbead cracking observed in multipass GTA plate welds on T-111 is grain boundary fracture. Phenomenologically, this is a typical high temperature failure mode in most metals, occurring usually at low strains although deformation adjacent to the grain boundaries may be quite extensive. The factors responsible for the observed grain boundary fracture are both metallurgical and structural in nature. First, T-111 possesses

* The term "underbead cracking", which is used throughout this report, is meant to describe cracks in plate welds located as shown in the sketch below:



good high temperature creep resistance, mainly as the result of solid solution strengthening of the matrix. Therefore, the relative difference in the matrix and grain boundary strengths may be more exaggerated than for some other refractory metal alloys at high temperatures. Secondly, lower melting alloying constituents, such as hafnium in T-111, tend to be concentrated at grain boundaries⁽⁴⁾; hence weakening them at high temperatures.

The objective of this program was to develop a modified filler metal composition and/or an improved GTA welding procedure which would reduce or eliminate grain boundary under-bead cracking in multipass GTA plate welds of T-111. A modified Varestraint test procedure was used early in the program to screen candidate filler metal compositions for basic weldability with regard to hot crack sensitivity. Further qualifications of selected filler metal compositions were judged on the results of manual, multipass GTA plate welds. Finally, the two most promising compositions were used in a comprehensive evaluation of alternate plate weld procedures and joint designs selected to minimize cracking both in the heat affected zone and base metal regions of the plate weldments.

3.0 PROGRAM AND PROCEDURES

3.1 TECHNICAL PROGRAM

The technical program for conducting a comprehensive weldability evaluation of T-111 plate as well as advancing the general state-of-the-art in the area of filler metals used in welding T-111 was divided into three tasks as schematically shown in Figure 1.

The first task of this program was directed toward the selection and preparation of various filler wire compositions. Eight compositions were selected which minimized the magnitude and differences in the elevated temperature strength of matrix and grain boundary regions. The importance of retaining useful mechanical properties and liquid alkali metal corrosion resistance in the experimental filler wire compositions was recognized.

The objective of Task II was the evaluation of the weld filler metal compositions prepared in Task I. Screening of the first eight filler metal for hot crack sensitivity was performed using a unique specimen design with the Varestraint test. Although all eight filler metals showed at least some cracking, four compositions were chosen, based on Varestraint data, for further evaluation using GTA multipass welds on 0.952 cm (0.375 inch) thick T-111 plate. A second series of five filler metal compositions was added to the program at this point to determine whether cracking could be eliminated even at the expense of drastic departure from the T-111 chemistry. Evaluation was done by both metallographic examination and mechanical testing of butt welds in plate.

The identification of improved GTA plate welding procedures and joint designs was the primary objective of Task III. To accomplish this, two filler metal compositions, which performed most satisfactorily in Task II, were used. Various joint designs including double "V", single "U", and single "V" (both with and without lands) were tried. Procedural variations incorporated were the number of passes, preheat, and restraint.

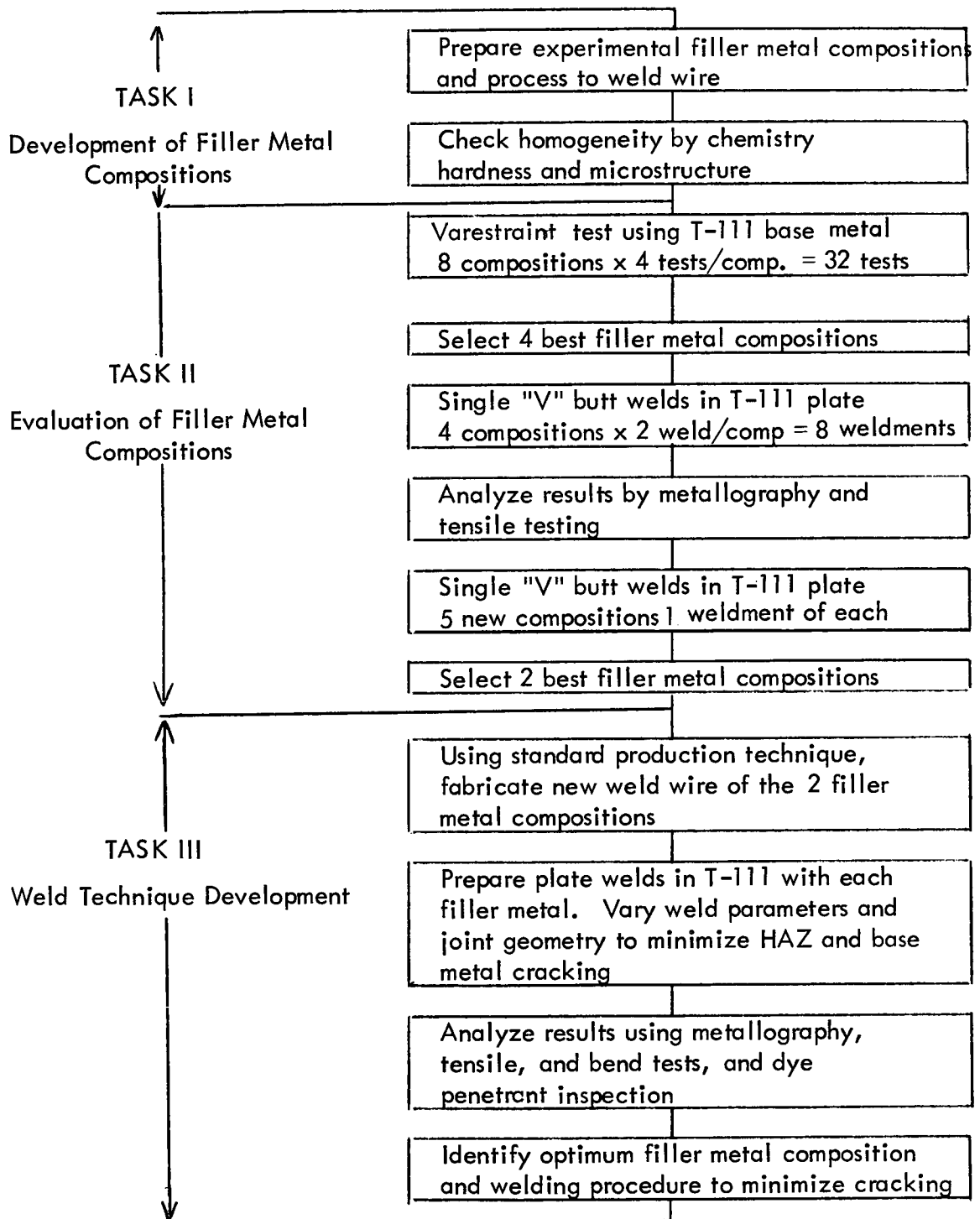


Figure 1. Program Outline

3.2 PROGRAM MATERIALS

The starting materials used to prepare the experimental filler wire compositions are listed in Table 1 along with the vendor supplied chemical analyses. Generally, Ta-10W was used as the base alloying ingredient to minimize any problems in mixing the very high melting point tungsten with the other alloying additions. Since only a limited amount of material was required for the Task II evaluations, the experimental compositions were prepared according to the following sequence:

- a. Starting sheet material was sheared, acid pickled, and weighed out as 0.7 kg charges.
- b. All charges were nonconsumable electrode DC arc melted as 7.62 cm (3 inch) diameter buttons in a purified argon atmosphere. The procedure used was to melt each button as completely as possible (generally 75-80% through), open the furnace, turn the buttons over, and remelt. Figure 2 shows the as-cast buttons.
- c. The buttons were warm rolled at approximately 371°C (700°F) to 0.127 cm (0.050 inch), sheared, pickled, and reloaded into the button melting furnace.
- d. Step b was repeated.

The nonconsumably arc melted buttons were warm rolled at 371°C (700°F) to a thickness of 0.254 cm (0.100 inch), annealed 1 hour at 1649°C (3000°F), and sheared to yield material suitable for the Task II evaluations. These evaluations required manual placement of filler metal on specially designed V-restraint test blanks of T-111. For this type of welding, the sheet material, sheared to narrow widths, was equally suitable as filler wire and, being easier to produce, was used for the Task II work.

To determine the homogeneity of the various filler metals, both chemical and metallographic analyses as well as hardness determinations on both the as-cast and rolled/annealed sheet material were performed.

Table 1. As-Received Chemical Analyses of Starting Material

Material	Heat No.	Vendor Analysis*								Filler Metal Used For
		Ta	Hf	W	Re	C	O	H	N	
Ta	600421	Bal.	--	--	--	< 30	< 50	3.1	10	1, 2, 3, 4, 5, 7, 8, 9, 10, 12, 13
Ta-10W	60B-758	Bal.	--	9.90	--	50	40	N/A	20	2, 3, 4, 7, 10, 11
W	C10-314	--	--	Bal.	--	< 20	< 20	N/A	< 30	1, 5, 8
Hf	410899	--	Bal.	--	--	< 30	< 50	N/A	50	1, 2, 3, 4, 5, 7, 8, 12, 13
T-111	650043	Bal.	2.0	8.2	--	< 40	90	2.9	12	6
Y	YM3-264	Not Available								6
Re	P-570	--	--	--	Bal.	6	38	N/A	10	8
T-111	613463	Bal.	2.0	7.9	--	40	40	10	40	Weld Blanks

* Metallic analyses in wt. percent. Interstitial (C, O, H, N) analyses in wt. ppm.

N/A = Not Available

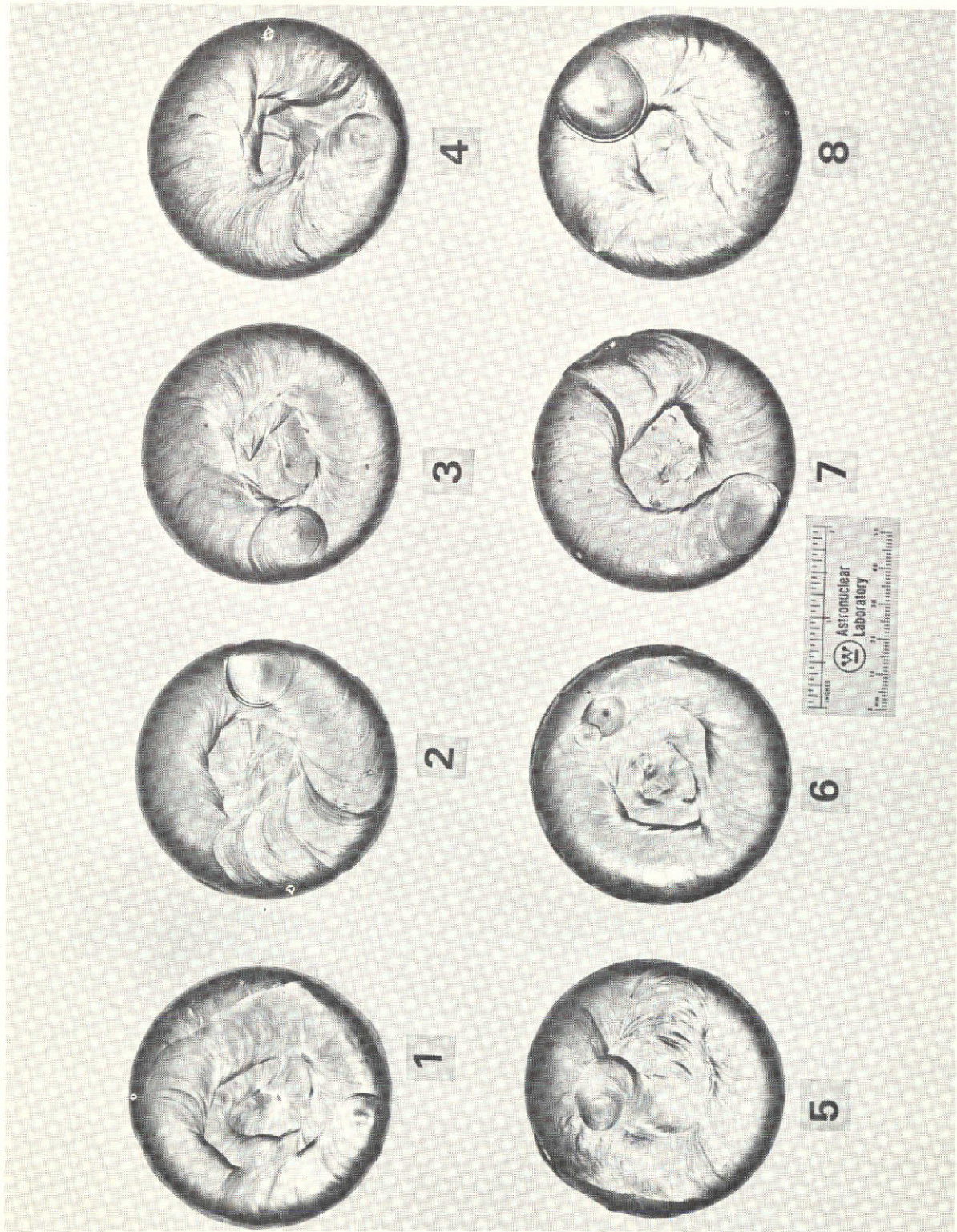


Figure 2. As-cast Buttons of Filler Metals 1 through 8

The first eight filler metals were analyzed for both major alloying constituents and interstitials. The results of these analyses are reported in Table 2. Concentrations of the intentional alloying additions were determined only for sheet material while the interstitial analyses for C, O, H, and N were performed on both as-cast and sheet material. Except for the observation that the analyzed tungsten content was generally lower than the nominal value, the chemistry results show the actual compositions are reasonably close to the nominal compositions. Of the 0.05 w/o yttrium added to the melt charge, chemical analysis indicated 0.04 w/o was retained through the melting and processing stages. Chemical analysis was not performed on the five filler metals added as a supplement to the original program.

The two most promising alloys, FM 4 (Ta-4W-1Hf) and FM 10 (Ta-4W), as judged from plate weld evaluations, were selected for use in the study of joint design and welding procedural effects. The filler metal wires for this phase of the program were manufactured using a procedure that would simulate a production scale operation. Two lots of each filler metal were made, each weighing about 2000 grams. Each charge was trough melted, flipped over, and remelted. The two charges of each filler metal were GTA welded together, consumable electrode melted, and cast into a 5 cm (2 inch) diameter mold. The resulting billets were machined to 3.78 cm (1.49 inch) diameter by 8.88 cm (3.5 inches) long and canned in mild steel. Each can was heated to 1200°C and extruded at a 3 to 1 reduction ratio. After the mild steel cans were chemically removed, the extruded billets were swaged at room temperature to 0.203 cm (0.080 inch) diameter. The filler wire was cut to length, chemically cleaned, and then vacuum annealed.

The chemical analysis results of the scale-up heats in Table 3 indicate excellent control of alloying additions and minimal interstitial pickup during the hot extrusion and vacuum annealing operations.

Table 2. Chemical Analyses of Filler Metal Compositions

Filler Metal Number	Nominal Composition (w/o)	Chemical Analysis ^(a)												
		As Cast				Rolled/Annealed Sheet								
		C	O	H	N	Ta	W	Hf	Re	Y	C	O	H	N
1	Ta-8W-1Hf	16	13	1.6	12	Bal.	8.0	0.96	-	-	17	15	1.3	5
2	Ta-7W-1.5Hf	35	5	1.5	15	Bal.	6.7	1.50	-	-	32	46	1.0	5
3	Ta-6W-1.5Hf	30	45	1.1	14	Bal.	5.6	1.48	-	-	34	48	1.1	14
4	Ta-4W-1Hf	33	19	1.6	14	Bal.	3.6	0.88	-	-	24	40	0.9	8
5	Ta-4W-2Hf	30	6	0.8	15	Bal.	3.8	1.95	-	-	8	17	0.9	4
6	Ta-8W-2Hf-0.05Y	21	5	1.1	24	Bal.	8.5	2.07	-	0.04	22	21	0.8	18
7	Ta-4W-3Hf-0.05C	535	7	0.8	13	Bal.	3.5	3.04	-	-	530	36	1.1	14
8	Ta-6W-0.8Re-1Hf-0.025C	270	8	0.8	11	Bal.	5.9	1.02	0.77	-	270	18	0.9	6
Typical T-111 Analysis		- - -				Bal.	8.0	2.0	-	-	< 40	50	< 1	10

(a) Metallic analyses in wt. percent.
 Interstitial analysis (C, O, H, N) in wt. ppm

Table 3. Chemical Analyses of Production Filler Metal Compositions

Filler Metal No.	Nominal Composition (w/o)	Chemical Analysis*										
		As-Cast				Extruded/Swaged Wire						
		C	O	H	N	Ta	W	Hf	C	O	H	N
4	Ta-4W-1Hf	32	17	0.5	11	Bal.	3.9	1.03	48	34	1.3	13
10	Ta-4W	21	32	0.9	8	Bal.	3.9	--	40	45	0.6	10

* Metallic analyses in wt. percent. Interstitial analyses (C, O, H, N) in wt. ppm.

The T-111 plate used as weld blanks in this program was excess material transferred from NASA Contract NAS 3-10602⁽³⁾. The chemical analysis of this material is listed in Table 1. The T-111 plate was conditioned and rolled at 426°C (800°F) to a thickness of 1.08 cm (0.425 inch) and then ground to the final thickness of 0.952 cm (0.375 inch). The specimens used for Varestraint tests came from the same plate; but instead of grinding to thickness, the plate was further rolled at 204°C (400°F) to a thickness of 0.318 cm (0.125 inch). Prior to vacuum annealing, the weld blanks were pickled in a 10% H₂SO₄, 15% HF, 20% HNO₃, 55% H₂O solution to remove any contamination resulting from prior fabrication processes. Following the pickling operation, the specimens were wrapped in tantalum foil and annealed for 1 hour at 1649°C (3000°F) at a pressure maintained in the 10⁻⁶ torr range. Besides annealing the specimens, this vacuum heat treatment served to further remove any residual hydrogen.

3.3 FILLER METAL COMPOSITION SELECTION

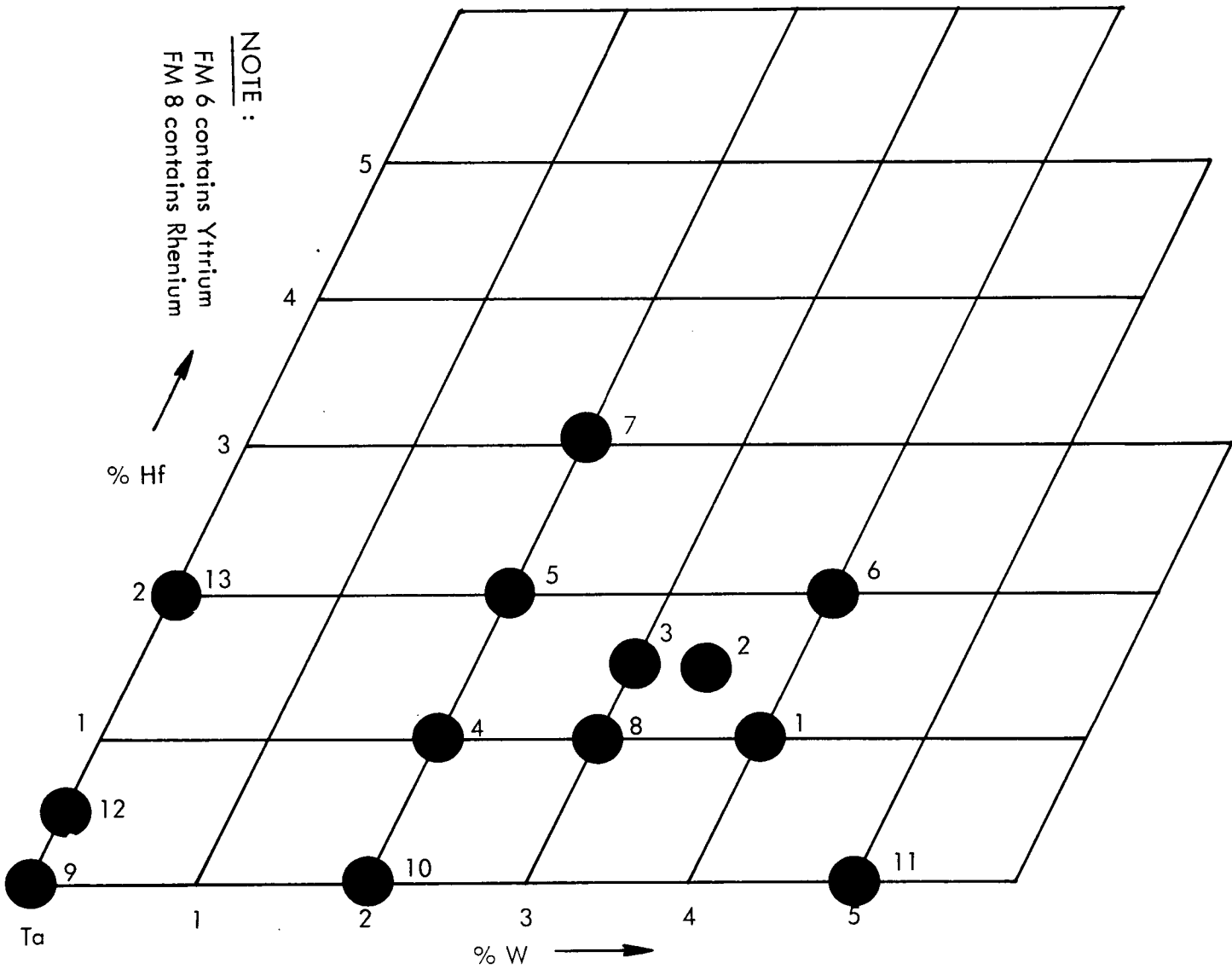
Filler wire compositions for evaluation were selected to change the structural and deformation characteristics of T-111 weld metal such that singly or in combination;

- The imbalance in matrix and grain boundary strengths at intermediate to high temperatures was lessened.
- Weld grain size was refined.

The thirteen filler metal compositions selected for study are listed in Table 4. The location of these compositions on the Ta-W-Hf phase diagram is shown in Figure 3 (neglecting yttrium and rhenium contents of compositions 6 and 8, respectively). Compositions 1 to 5 were selected to investigate the region between the crack-prone T-111 (Ta-8W-2Hf) and crack-free Ta and Ta-10W compositions. Yttrium was added to the sixth composition in order to refine the grain size. Compositions 7 and 8 were selected to permit evaluation of a high interstitial level alloy and a near ASTAR-811C composition, respectively.

Table 4. Nominal Filler Metal Compositions

Filler Metal Number	Nominal Composition (wt. %)
1	Ta-8W-1Hf
2	Ta-7W-1.5Hf
3	Ta-6W-1.5Hf
4	Ta-4W-1Hf
5	Ta-4W-2Hf
6	Ta-8W-2Hf-0.05Y
7	Ta-4W-3Hf-0.05C
8	Ta-6W-0.8Re-1Hf-0.025C
9	Ta-unalloyed
10	Ta-4W
11	Ta-10W
12	Ta-0.5Hf
13	Ta-2Hf



(Note: Numerals adjacent to each dot represent filler metal number)

Figure 3. Location of Nominal Filler Metal Compositions on the Ta-W-Hf Ternary Phase Diagram

ASTAR-811C has been shown to be less sensitive to underbead cracking than T-111, and yet it retains the desired strength and corrosion resistance⁽¹⁾.

Compositions 9 through 13 were included to determine whether crack-free welds could be made in T-111 plate without regard for mechanical or corrosion properties. Hence, compositions 9 through 11 contain no Hf while compositions 12 and 13 are tungsten-free.

3.4 VARESTRAINT TESTING

The first eight filler metal compositions were screened using the recently developed Varestraint test which establishes a quantitative measure of the ability of weld metal to accommodate superimposed strain at elevated temperatures. The principle and operation of the Varestraint test has been reviewed in detail in past programs^(5,6). While the Varestraint test does not reproduce the "underbead cracking" observed in plate welds it is valuable in screening materials for classic hot cracking tendencies. Further, since the precise cause(s) of the plate weld cracking are not known, it was hoped some correlation with hot crack propensity could be identified.

A photo of the Varestraint apparatus is shown in Figure 4, and the various parts are tagged. Both the specimen and the fixture were placed inside the weld chamber which was evacuated and backfilled with ultra-high purity helium. Both the oxygen and water vapor levels within the chamber were constantly monitored, each being maintained below 5 ppm.

The specimens were tested and unloaded while in the chamber, thus eliminating the need to reload the chamber following each test. During the test an arc was struck on each loaded specimen. The arc moved automatically along the plate until reaching a triggering mechanism which immediately activated the bending mechanism and then shut off the arc as shown in Figure 5.

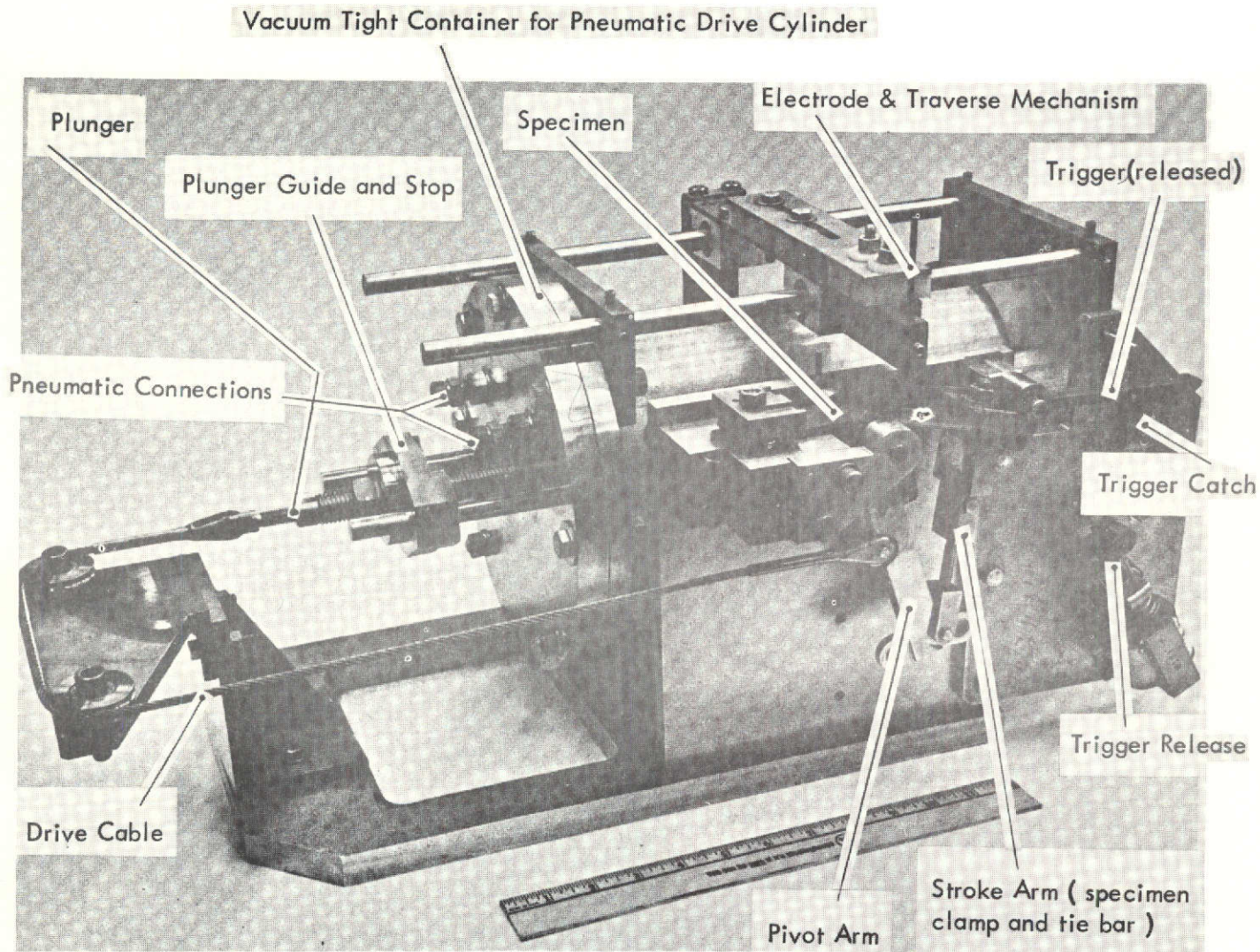


Figure 4. Varestaint Test Apparatus

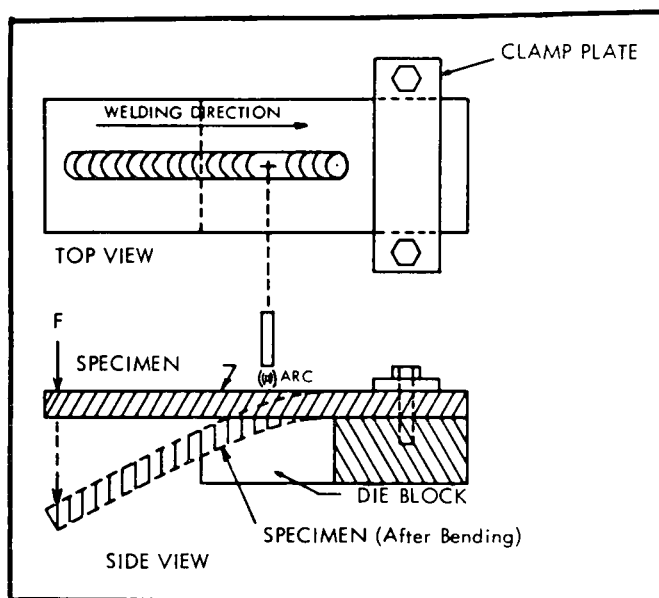


FIGURE 5 - Schematic: Bending Technique for Augmenting Strain by Restraint Testing

The total outer fiber strain imposed on the specimen is calculated by the following formula:

$$\text{Strain} = \frac{t}{t + 2R} \approx \frac{t}{2R}$$

where: t = specimen thickness

R = die block radius

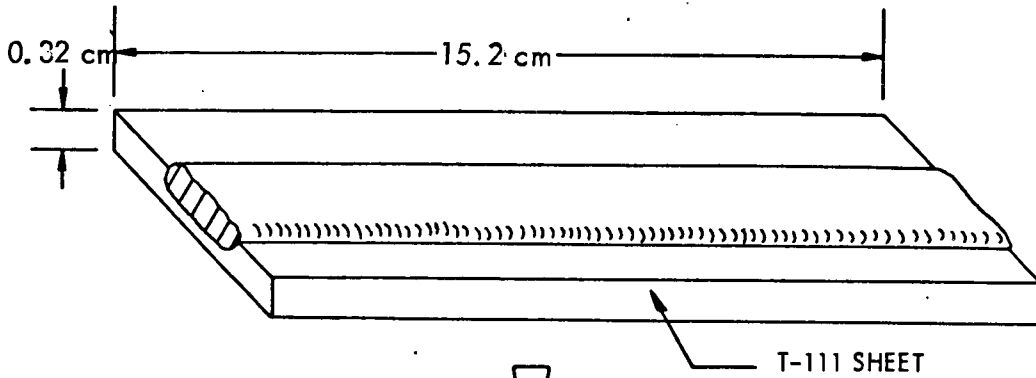
Specimens for the first eight filler metal compositions were prepared for Varestraint testing as shown in Figure 6. A weld metal layer was deposited for each filler metal composition on T-111 specimen blanks. The specimens were then surface ground to insure that the weld bead would be uniform and flat. These blanks were then Varestraint tested using the procedures established on Contract NAS 3-11827⁽⁵⁾. The preplaced weld metal layer was of sufficient size to completely contain the Varestraint weld pass. Hence, this was a test of as-cast and diluted weld metal. By using the T-111 containment substrate, the test became a realistic replacement of actual weld conditions with regard to chemical composition gradients in the base metal-filler metal interface region. Three specimens were used for each filler metal composition. These specimens were then tested at various predetermined strain levels of 2, 3, and 4%.

3.5 BUTT WELDING EVALUATION

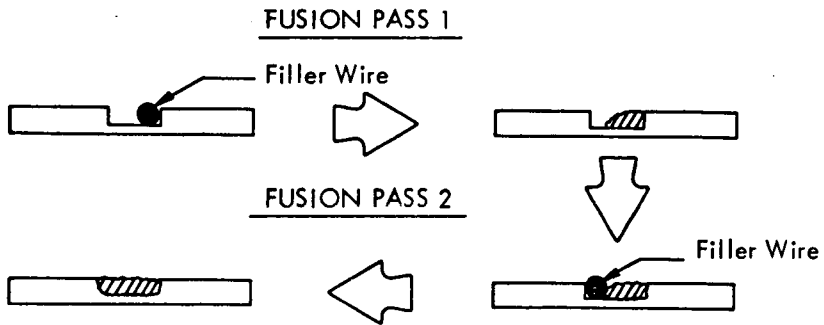
3.5.1 Initial Series (Welds 1-13; Single "V" Configuration)

The four most promising filler metal compositions of the first eight compositions were selected for use in the preparation of butt weld joints. The filler metals chosen were FM 3 (Ta-6W-1.5Hf), FM 4 (Ta-4W-1Hf), FM 5 (Ta-4W-2Hf), and FM 8 (Ta-6W-0.8Re-1Hf-0.025C). Additional plate welds were prepared using FM 9 (Ta), FM 10 and 11 (Ta-W alloys; no Hf), and FM 12 and 13 (Ta-Hf alloys; no W).

AS FABRICATED FILLER WIRE VARESTRAINT SPECIMEN



PREPLACED WELD BEAD OF EXPERIMENTAL FILLER WIRE COMPOSITION.
WELD BEAD PREPARED AS SHOWN BELOW :



VARESTRAINT TEST

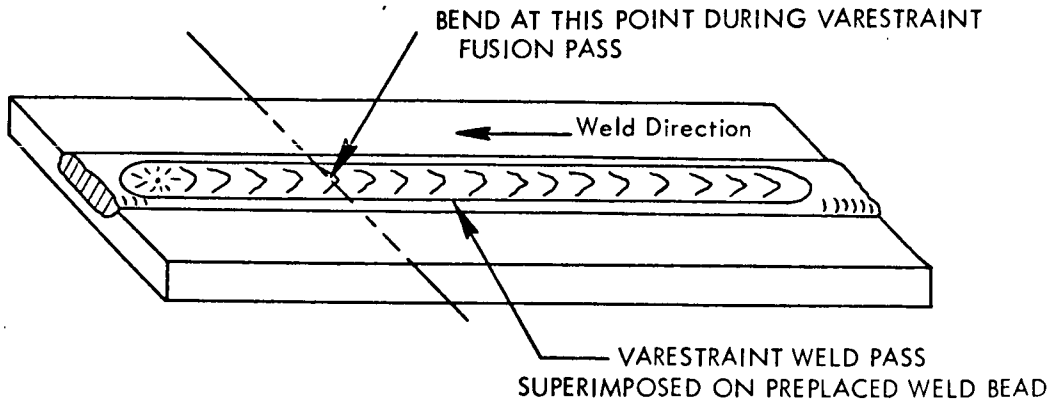


Figure 6. Preparation and Test Concept for Vareststraint Evaluation of Filler Wires

Two joints of the single "V" configuration, shown in Figure 7, were made using each of the four Varestraint tested compositions. One joint was made of each of the five additional compositions for a total of 13 welded joints. Welding was done manually using 9 to 12 passes including the root pass. During welding the T-111 plate weld blanks were clamped in a restraining fixture. The fixtured weld was mounted on a traversing table which permitted a uniform, reproducible welding speed of 25.4 cm/min (10 in/min.) to be used. Prior to welding, both the filler metal and the weld blanks were pickled and vacuum annealed to remove any contamination which might have influenced the weld integrity.

The weld chamber was evacuated and backfilled with ultra-pure helium prior to welding. Oxygen and water vapor levels were maintained at less than 5 ppm, averaging about 1 ppm. All welding was done using straight polarity direct current (SPDC). The electrodes were made of 0.24 cm (0.094 inch) diameter centerless ground 2% thoriated tungsten which had been ground to a blunted 0.079 cm (0.031 inch) diameter tip.

Prior to welding, the specimens were placed in the molybdenum jaws of a fixture which provided both positioning during welding and restraint against the inherent weldment deformation. The root faces were in contact, and no gap was permitted. The root pass for the initial 13 weldments was made by fusing the root of the joint without filler metal addition. Hence, the composition of the root pass weld was that of the T-111 base metal.

The single "V" butt weld joint design and the welding procedures initially used did not represent an attempt to optimize either with respect to weld cracking. They were selected mainly because they represented conditions for which the bulk of the experience on the underbead cracking has been accrued and also represent reasonable conditions for most actual hardware-type field welding operations. Limited experience has, however, shown other weld geometries to be somewhat less prone to cracking⁽³⁾, although some of these are not compatible with normal hardware fabrication techniques. Also, some lessening of

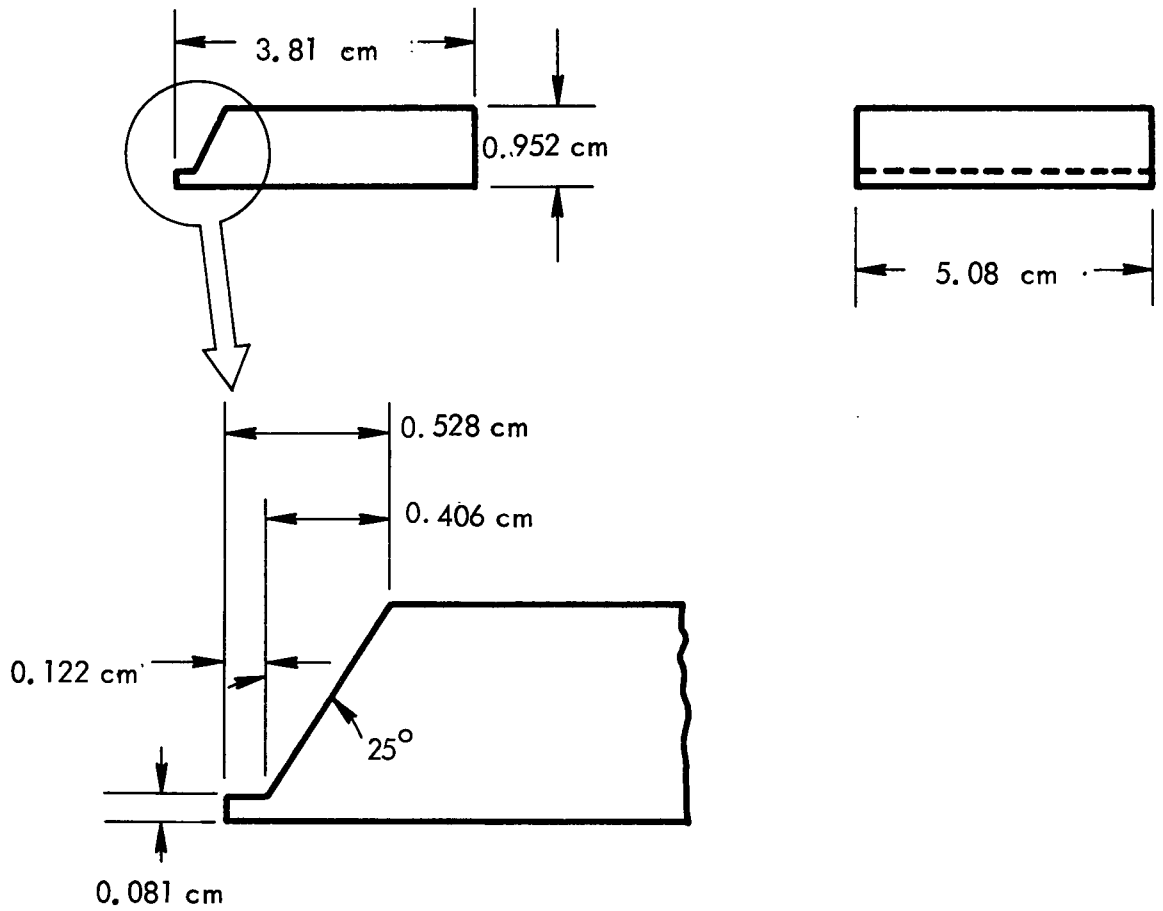


Figure 7. Configuration Used for Single "V" Plate Welds

the underbead cracking problem has been observed in T-111 plate welds by use of certain procedural variations⁽¹⁾. Thus, efforts to optimize both the weld joint design and welding procedures were undertaken.

3.5.2 Second Series (Welds 14-29; Varied Configurations)

Included in the plate welding parameters evaluated were welding speed, weld joint geometry, weld restraint, and filler metal deposition rate. Control of the welding speed and weld deposition rate, in turn, control the heat input per unit weld length. Detailed logistics were maintained for each of the welds prepared.

Three different weld joint geometries were fabricated and welded. A sketch of the single "U" design is shown in Figure 8. This configuration results in a relatively "tight" joint. Significantly less filler metal is required to fill such a joint, and, therefore, the number of passes and heat input can be greatly reduced. The other design used was a double "V" groove of two types as shown in Figure 9. The Type I design was tried first because the root faces allowed for root passes without the use of filler metal. However, initial welds indicated inadequate penetration in the root areas resulting in unwelded areas. By using the Type II design and filler metal in the root pass this difficulty was avoided.

For plate welds of both the initial (welds 1-13) and second (welds 14-29) series, the presence of underbead cracking was established metallographically by examining sections of each weld. A comparison of the effects of the various metal compositions and weld parameters was established based upon the effectiveness in eliminating cracking in the weld metal area, heat-affected zone, and base metal. Specimens were prepared for examination using standard metallographic techniques. The etchant used to reveal the microstructure and to remove smeared metal was a solution containing by volume 40% HCl-40% HF-20% HNO_3 . The specimens were swabbed with the etchant for about 15 seconds then thoroughly rinsed and dried. The duration of application and the etchant strength are of prime importance since the grain boundary areas

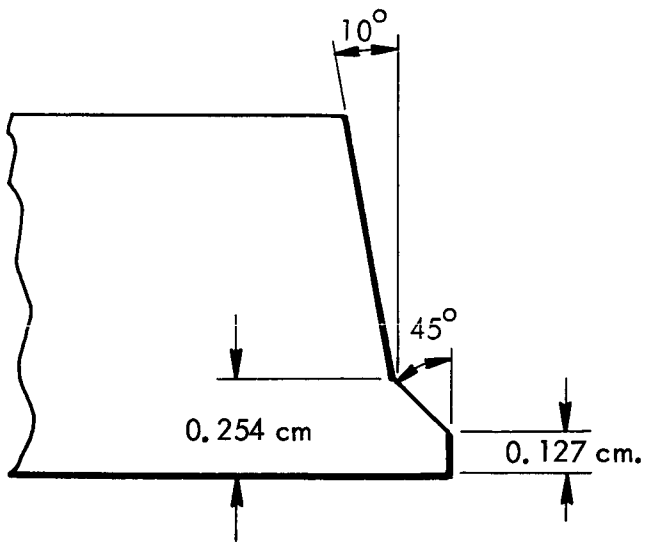
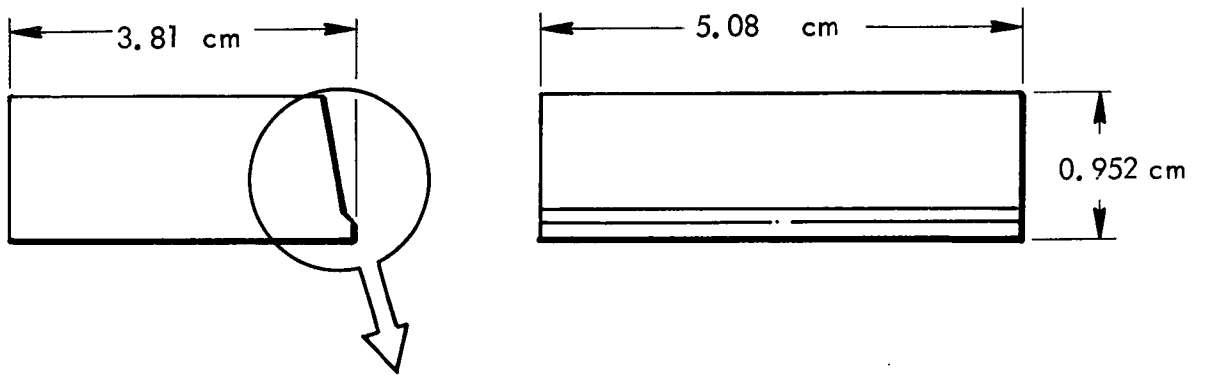


Figure 8. Configuration Used for (Modified) Single "U" Plate Welds

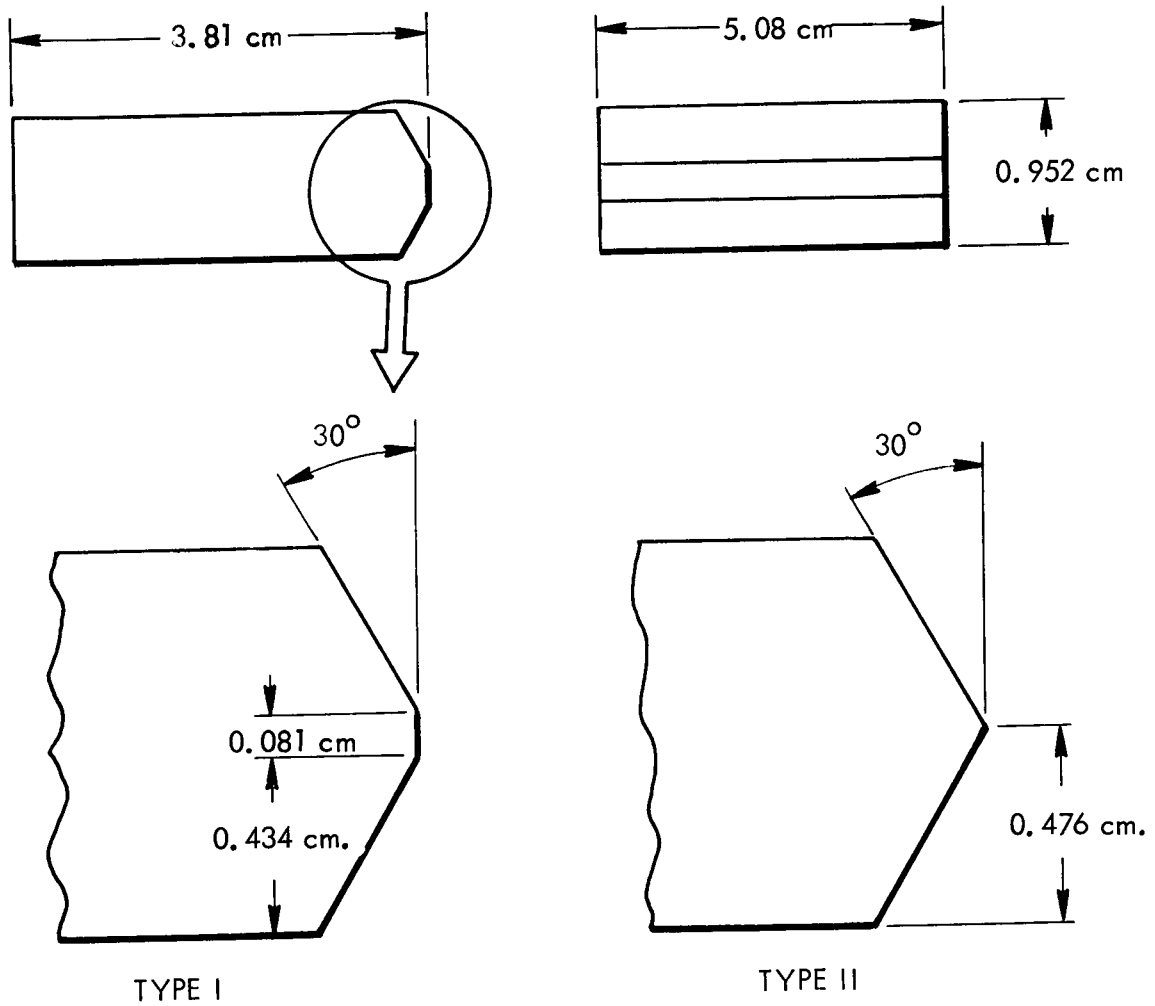


Figure 9. Configurations Used for Double "V" Plate Welds

of the T-111 weldments are rapidly attacked. This slightly preferential attack sometimes resulted in false signs of grain boundary cracking. In fact, some of the very small "cracks", which appear to be a coalescing of voids within the grain boundary, are not evident in the as-polished condition and are only observed in the fully etched condition. These "cracks", which become more distinct if the etchant is allowed to react for greater periods, are best classified as grain boundary voids which may have resulted from the specimen preparation rather than being inherent cracks within the weldment.

Tensile tests were performed at room temperature and 1649°C (3000°F) on specimens of the initial series of welds (1-13) and at room temperature on specimens of the second series (welds 14-29). The tensile specimen, Figure 10, was relatively small due to the size of the weld blank. The round bar tensile specimens were machined to have the weld zone transverse to the longitudinal axis of the tensile specimen as shown in Figure 10. These specimens provided comparative data on the mechanical strength and ductility of the various filler metals and weldments. Note in Figure 10 that the cracked region was generally below the reduced section. A factor which should be considered in the interpretation of the tensile is that, due to the fact the specimens were removed from the same location in each weld whereas the extent and severity of cracking varied in the welds, rigorous comparisons should be avoided.

Bend tests were performed on test weldments 18 through 24, which had been prepared with filler metals FM 4 (Ta-4W-1Hf) and FM 10 (Ta-4W). These were done to further evaluate weld quality; i. e., soundness and ductility of the weldment. The bend specimens were 5.08 cm (2 inches) long and 0.952 cm (0.375 inch) wide and thick. The face and root surfaces of the weldment were not ground prior to testing. The bend tests were made using a 1 t punch radius and a punch speed of 2.54 cm/min. (1.0 in/min.). A three point bend fixture was used with a major span of 5.08 cm (2.0 inches). Except where noted in the Discussion, bends were performed with the weld face in tension.

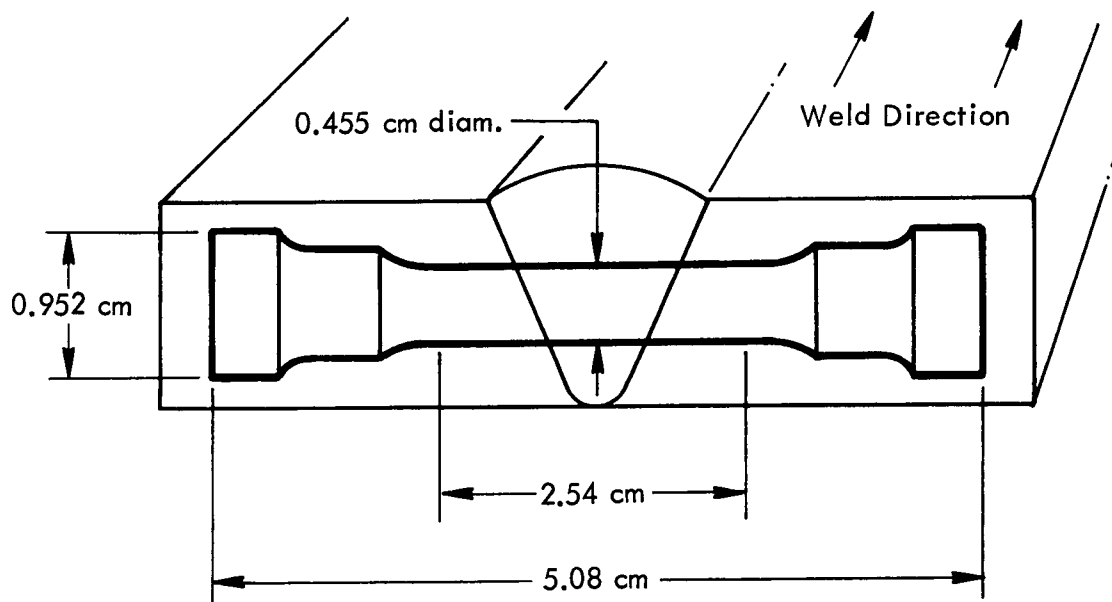


Figure 10. Schematic : Orientation of Tensile Specimens
Within Plate Welds

As supplements to the mechanical tests, electron beam microprobe analyses and hardness traverses were made to determine the extent of segregation and the variation in weld strength (hardness) within the weld zone. The electron beam microprobe unit was set to count back-scattering at the hafnium wave length. Various areas within the weld were scanned and the relative concentration of hafnium recorded. The beam was typically 1 micron in diameter thus permitting the sampling of very localized areas. The hardness readings were taken on a Vickers diamond pyramid hardness tester using 10 or 30 Kg load.

4.0 RESULTS AND DISCUSSION

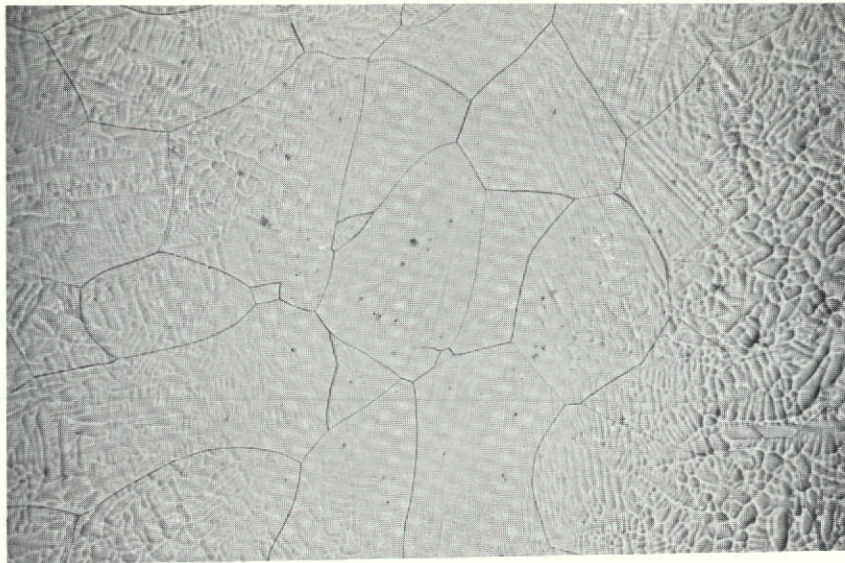
4.1 FILLER METAL CHARACTERIZATION

Metallographic examination was performed on both as-cast and rolled/annealed material of all filler metal compositions. The as-cast structures of all compositions were typical of material prepared in this way. Grain size was quite large, and evidence of the dendritic solidification mode was abundant. With the exception of the more complex alloys (FM 6-8) the microstructures were single phase in appearance. The as-cast structure of FM 3 (Ta-6W-1.5 Hf), typical of all but FM 6-8, is shown in Figure 11 as is that of FM 6 (Ta-8W-2Hf-0.05Y). The as-cast structures of FM 7 (Ta-4W-3Hf-0.05C) and FM 8 (Ta-6W-0.8Re-1Hf-0.025C) are shown in Figure 12. The obvious differences in precipitate morphology imply that the precipitates are of different composition and/or crystal structures.

Typical microstructures of FM 4 (Ta-4W-1Hf) and FM 8 (Ta-6W-0.8Re-1Hf-0.025C) in the rolled/annealed condition are shown in Figure 13. FM 4 is typical of all but FM 7 and 8. Both FM 7 and 8 had the expected intragranular precipitate network typified by FM 8, Figure 13.

Results of metallographic examinations of the rolled and annealed filler metal compositions indicated the following:

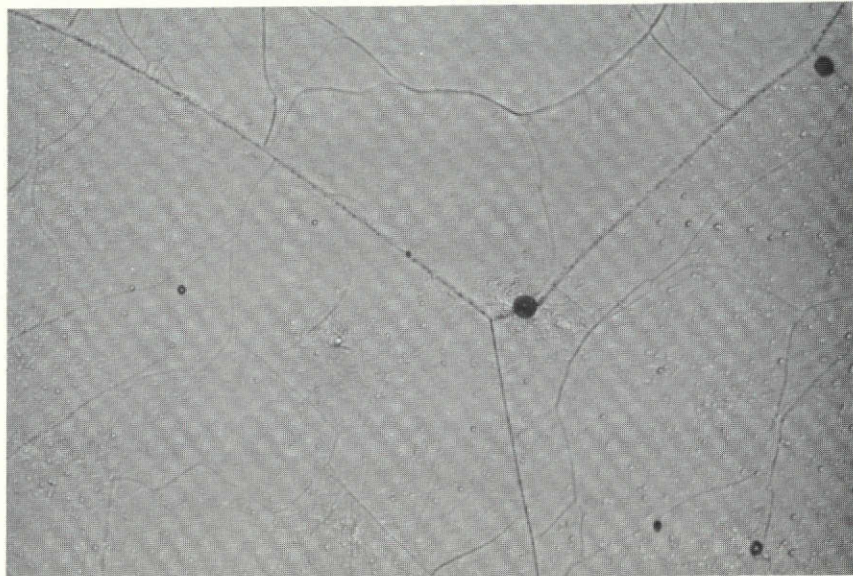
- The rolling process did not result in sufficient deformation to fully recrystallize all alloys in the 1 hour - 1649°C (3000°F) anneal employed.
- In the solid solution alloys, the heterogeneity of the deformation led to a duplex grain size after the 1 hour - 1649°C (3000°F) anneal.
- The presence of yttrium in FM 6 appears to retard recrystallization. The resulting grain size is often small but quite irregular.



50X

Ta-6W-1.5Hf

FM 3

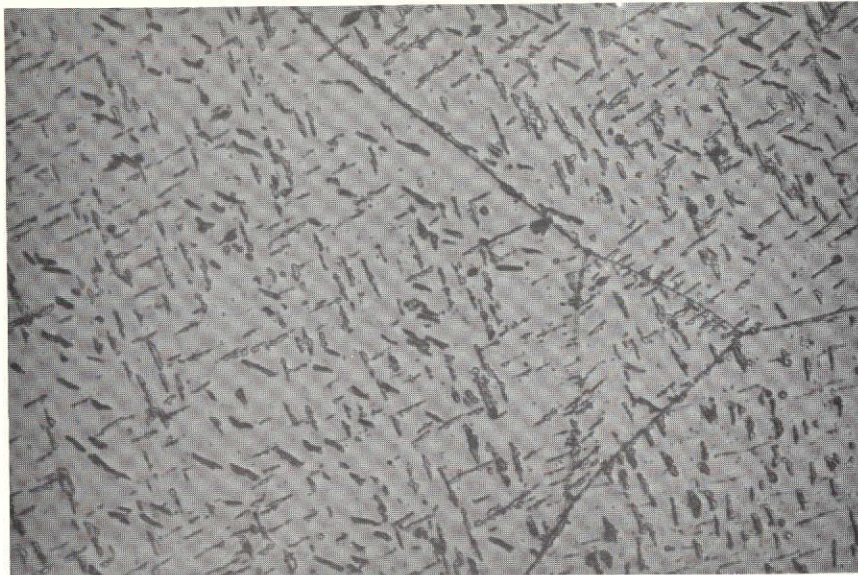


50X

Ta-8W-2Hf - 0.05Y

FM 6

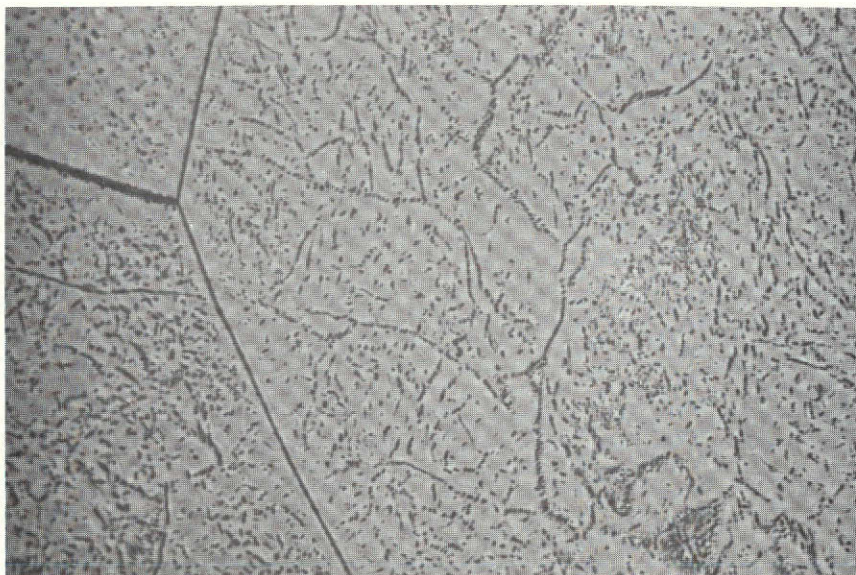
Figure 11. As-Cast Microstructures - FM 3 and 6



400 X

Ta-4W-3Hf-0.05C

FM 7

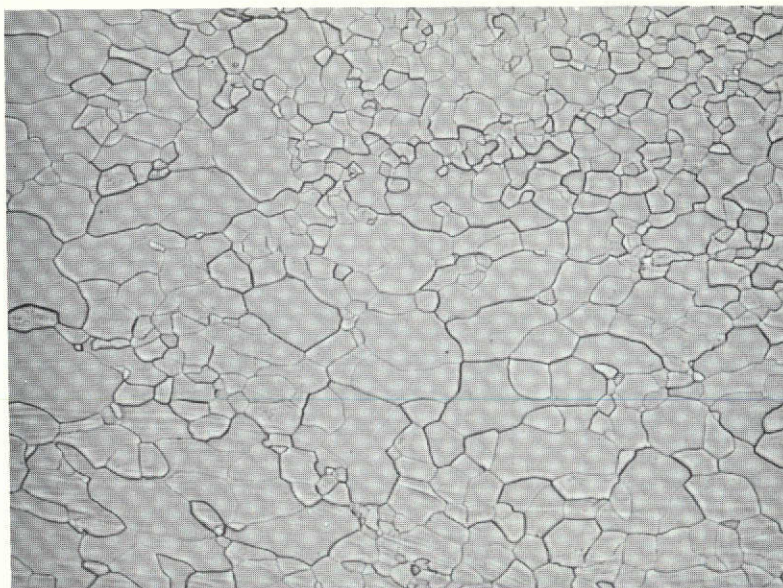


400 X

Ta-6W-0.8Re-1 Hf-0.025C

FM 8

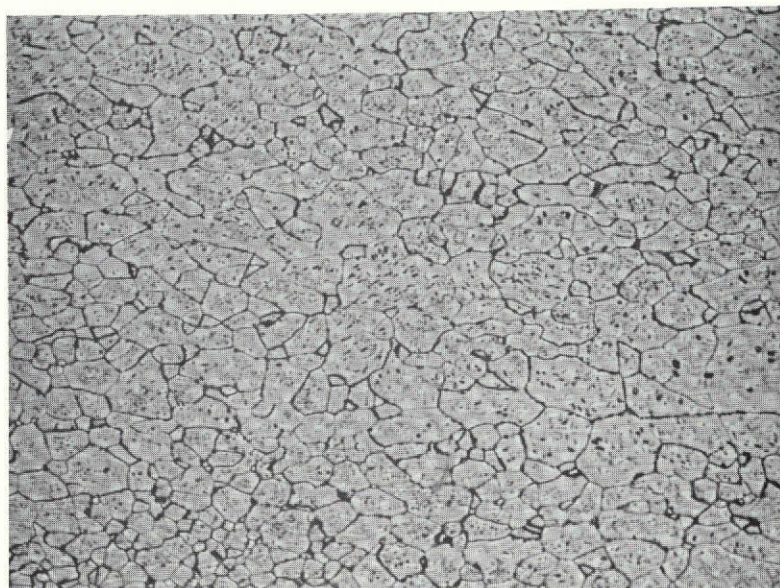
Figure 12. As-Cast Microstructures - FM 7 and 8



100 X

Ta-4W-1 Hf

FM 4



100 X

Ta-6W-0.8Re-1 Hf-0.025C

FM 8

Figure 13. Typical Rolled/Annealed Microstructures - FM 4 and 8

- FM 7 and 8 exhibit small grain size. In FM 7, in particular, the grains are quite equi-axed.

The as-cast and rolled/annealed hardness was determined for each of the first eight filler metals while only the rolled/annealed hardness was measured for filler metals 9 through 13. These data are reported in Table 5.

Along with the average hardness, \bar{X} , Table 5 also lists the standard deviation, S , and the number of observations, N . The standard deviation can be considered as an indication of the relative homogeneity of the material. Unalloyed tantalum, FM 9, has a relatively low S of 1.51 which is interpreted as meaning a homogeneous structure. On the other extreme is FM 13 (Ta-2Hf) with an S of 7.2 indicating the possibility of varying hafnium concentration within the structure.

The relative effects of additions to solid solution strengthened alloys are shown by the difference in reported hardness readings. Both tungsten and hafnium are solid solution strengtheners of tantalum.⁽⁷⁾ Of these two, hafnium is by far the more potent because of its limited solubility. As an example, using the hardness of FM 9 (pure tantalum) as a basis, additions of 2% hafnium (FM 13) and 4% tungsten (FM 10) result in nearly equal hardness increases. Even 0.5% hafnium (FM 12) increases the hardness of tantalum by 25%.

The manufacture of production scaled lots of FM 4 (Ta-4W-1Hf) and FM 10 (Ta-4W) for the welding procedure variation studies was successfully completed using the previous discussed operations of double trough melting, consumable electrode casting, extruding, and swaging. A wire diameter of 0.203 cm (0.080 inch) was determined to be optimum for these welding applications. Wire of larger cross section more rapidly cooled the weld pool resulting in a tendency for unwelded areas. Smaller cross section wires were more difficult to manipulate when trying to fill the joint in a minimum number of passes.

Table 5. Results of Hardness Measurements on Filler Metal Compositions

Filler Metal No.	Nominal Composition (w/o)	Vickers (Diamond Pyramid) Hardness					
		As-Cast*			Rolled/Annealed Sheet**		
		\bar{X} (DPH)	S	N	\bar{X} (DPH)	S	N
1	Ta-8W-1Hf	199.2	6.34	18	191.2	3.97	6
2	Ta-7W-1.5Hf	209.2	5.20	20	189.0	3.16	6
3	Ta-6W-1.5Hf	198.6	5.81	20	181.5	3.50	6
4	Ta-4W-1Hf	158.2	3.91	20	144.8	2.78	5
5	Ta-4W-2Hf	164.8	4.19	19	159.3	4.46	6
6	Ta-8W-2Hf-0.05Y	227.5	5.55	19	228.6	3.46	5
7	Ta-4W-3Hf-0.05C	219.0	5.84	19	194.0	4.76	6
8	Ta-6W-0.8Re-1Hf-0.025C	253.8	3.36	18	215.3	6.86	6
9	Ta-unalloyed	N/A	N/A	N/A	79.0	1.51	6
10	Ta-4W	N/A	N/A	N/A	153.5	2.4	4
11	Ta-10W	N/A	N/A	N/A	195.2	6.1	6
12	Ta-0.5Hf	N/A	N/A	N/A	100.2	2.6	6
13	Ta-2Hf	N/A	N/A	N/A	147.5	7.2	6

* 30 Kg (294.2 N) Load Used

S - Standard Deviation

** 10 Kg (98.06 N) Load Used

N - Sample Size

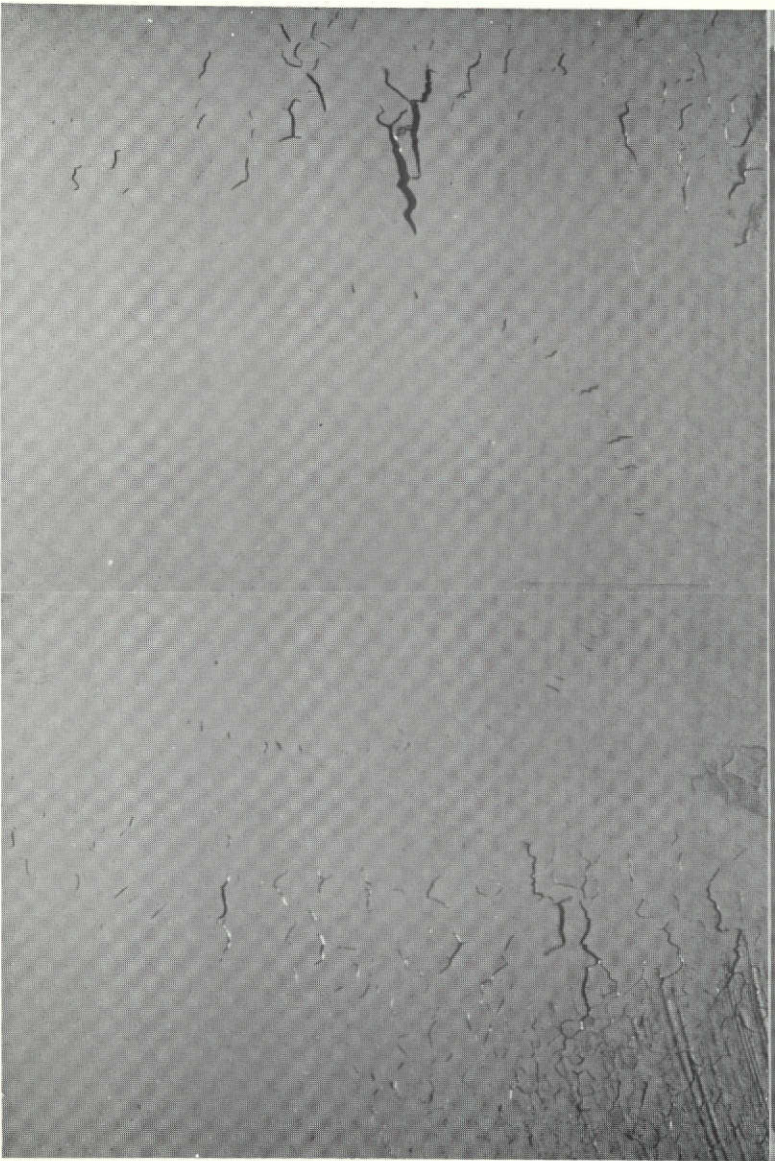
4.2 VARESTRAINT RESULTS

Three specimens of each of the first eight filler metal compositions were tested. The augmented strain levels used were 2%, 3%, and 4%. All specimens were tested using a 0.635 cm/sec (15 IPM) welding speed and 205 amps weld current.

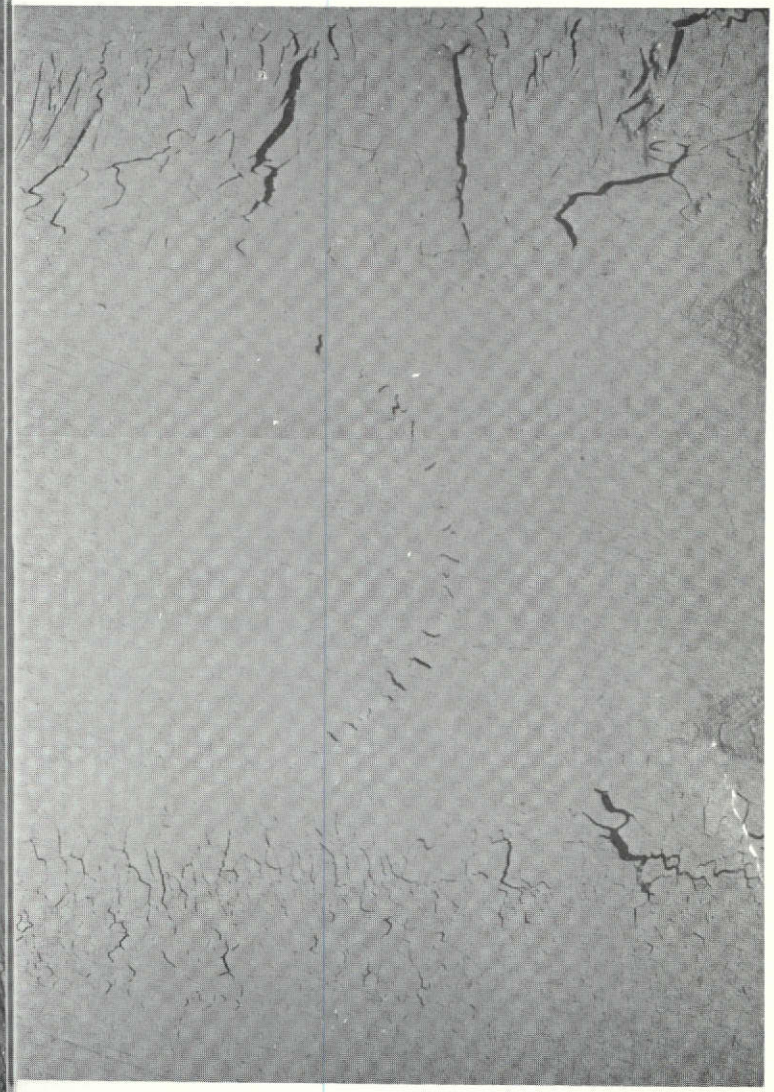
The total crack length was determined for each specimen using three different techniques. The amount of cracking in the weld fusion zone was determined both on the as-tested specimens and after the surface of the specimens had been lightly polished and etched. Previous experience has shown the latter procedure makes it easier to distinguish cracks from grain boundary grooves and folds which also result from the testing. It does, however, suffer from the difficulty in removing precisely the same amount of material; i. e., going to the same depth, in all specimens.

The third total crack length count was made on cracks in the "heat affected zone". This heat affected zone, due to the unique specimen design employed, consists of as-cast filler metal deposited during the preliminary specimen preparation. Normally, cracking in the HAZ during Varestraint testing is ignored in the analysis of the data. However, in the present program this cracking seemed more important. First, the amount of cracking was, in general, considerably greater than had been observed in the past⁽⁵⁾. This undoubtedly stems from the fact that the HAZ regions of the present Varestraint specimens consist of very large grained, as-cast material, whereas prior tests have been on wrought, recrystallized sheet material. Also, the nature of the underbead cracking problem, which is the subject of this study, implies this type of cracking -- along grain boundaries during high temperature straining -- may be of more direct importance.

Typical crack patterns for several filler metals are shown in Figures 14 and 15. The specimens were polished prior to being photographed. The length of each crack was optically measured

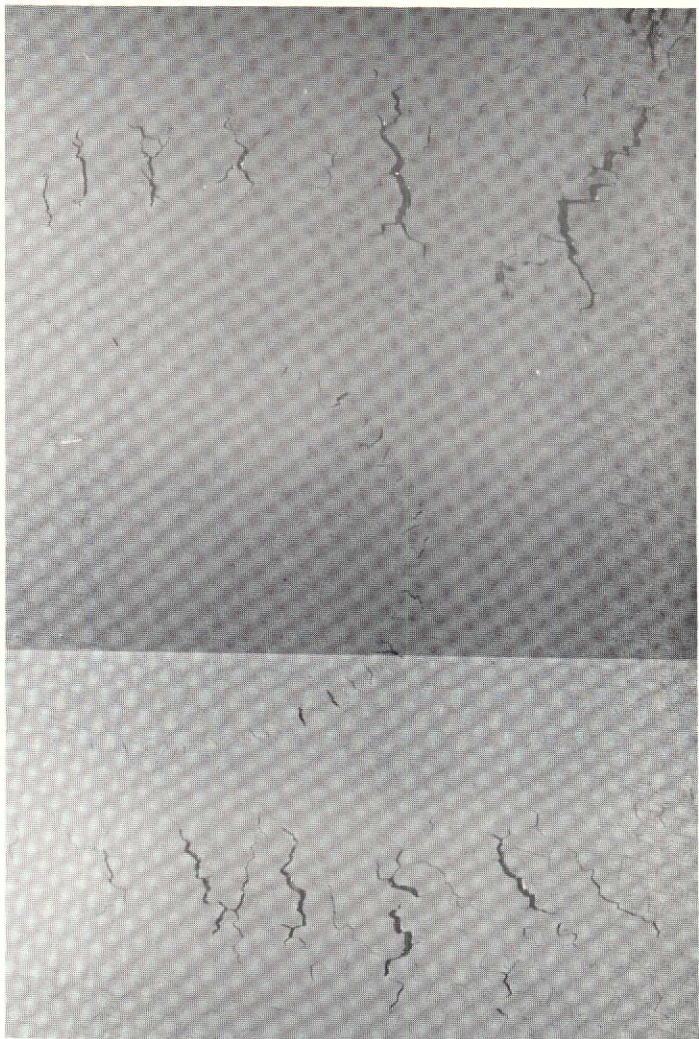


FM 1 Ta-8W-1Hf 3% Strain

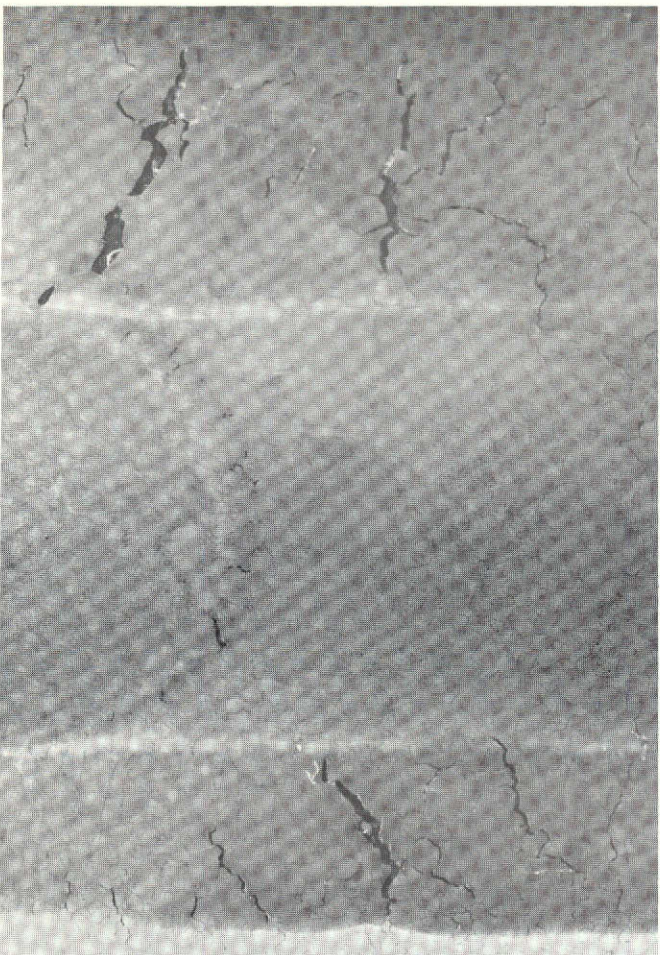


FM 6 Ta-8W-2Hf-0.05 Y 3% Strain

Figure 14. As-polished Vareststraint Crack Patterns in FM 1 and FM 6



FM 8 Ta-6W-0.8Re-1Hf-0.025C 4% Strain



FM 7 Ta-4W-3Hf-0.05C 4% Strain

Figure 15. As-polished Varestraint Crack Patterns in FM 7 and FM 8

using a microscope with a calibrated filar eyepiece. The HAZ cracks, which are located in previously deposited weld metal, show up as the large cracks nearer the sides of the specimens. The fusion zone cracks are those forming a small crescent in the center area. The filler metal crack patterns shown are not typical of all filler metals tested; in fact, the structures depicted in these fixtures are those most sensitive to cracking. The best filler metal, FM 4 (Ta-4W-1Hf), had less than 1/3 the amount of cracks of FM 1 (Ta-8W-1Hf), the best of the four shown.

The complete results of the Varestraint tests are presented in tabular form in Table 6. This data is provided for completeness, but it is obvious that the large number of variables and data presented make it difficult to concisely review the results. The more important results would seem to be:

- The HAZ cracking is by far the most severe both in number and in length.
- The effect of higher strain is to increase both the number and length of the cracks. A plot of strain versus total crack length generally produces a uniform curve, varying in form from linear to exponential depending upon the filler metal.
- There is not a large difference between the filler metals in the extent of their fusion zone cracking. The HAZ data determined the relative susceptibility to cracking of each filler metal. Since cracking in the HAZ Varestraint specimen most closely approximates the underbead cracking in GTA welds, the inclusion of the HAZ data in the analysis to determine the best filler metal is justified.

The data of Table 6 are presented in summary form in Table 7. The values reported in Table 7 represent the total of all crack length measurements for the particular combination of strain and filler metal; i. e., fusion zone (as-tested) plus fusion zone polished and etched plus

Table 6. Vareststraint Crack Count Data

FM No.	% Strain	Fusion Zone Cracks						HAZ Cracks		
		As-Tested			Polished & Etched			TCL* m x 10 ⁵	MCL** m x 10 ⁵	No.***
		TCL* m x 10 ⁵	MCL** m x 10 ⁵	No.***	TCL* m x 10 ⁵	MCL** m x 10 ⁵	No.***			
1	2	7.4	7.4	1	N/A	N/A	N/A	N/A	N/A	N/A
	3	199.	34.3	15	236	22.9	26	1450	135	55
	4	142.4	26.2	12	345	45.7	25	1400	137	39
2	2	22.9	16.0	2	64.0	12.6	9	528	76.2	43
	3	99.1	17.8	10	22.4	17.8	24	2290	178	84
	4	195.	20.6	15	305	22.9	20	564	83.8	33
3	2	0	0	0	65.6	13.7	8	765	50.8	57
	3	150.	12.7	19	229	25.4	20	889	71.1	48
	4	236.	27.9	17	351	35.6	20	1800	107	51
4	2	0	0	0	0	0	0	236	33.0	20
	3	86.4	20.3	8	206	35.6	16	292	35.6	21
	4	234.	25.4	15	157	27.9	12	43.2	12.7	5
5	2	9.14	9.14	1	54.9	13.7	6	165	35.6	14
	3	112.	20.3	10	257	33.0	27	965	60.9	45
	4	165	17.8	13	272	30.5	18	262	61.0	11
6	2	0	0	0	62.7	11.4	9	1760	68.6	107
	3	107	20.3	9	218	22.8	18	2490	173	166
	4	241	27.8	16	305	30.5	20	2180	239	39
7	2	0	0	0	127	17.1	13	5330	127	270
	3	224	22.9	15	239	43.1	17	3990	188	83
	4	353	30.5	22	314	35.6	17	5440	216	126
8	2	37.3	10.3	2	101	13.7	11	983	117	38
	3	137	15.3	13	348	25.4	31	1900	78.7	86
	4	170	25.4	12	281	22.9	21	2320	157	66

* TCL - Total Crack Length
 ** MCL - Major Crack Length
 *** No. - Number of Cracks

Table 7. Summary of Vareststraint Data

Filler Metal No.	Total Crack Lengths					
	2%		3%		4%	
	meters (x 10 ³)	(mils)	meters (x 10 ³)	(mils)	meters (x 10 ³)	(mils)
1	N/A	N/A	18.7	735	19.3	760
2	6.15	242	21.1	830	10.8	425
3	8.33	328	13.0	510	23.6	930
4	2.36	93	5.72	225	5.84	230
5	2.29	90	11.9	470	6.86	270
6	18.3	719	27.4	1080	27.7	1090
7	54.6	2150	45.5	1790	57.66	2270
8	11.0	435	23.7	935	27.4	1080

N/A = Not Available

Data reported above includes all data from Table 6.

HAZ cracks. One of the most striking results observed is the very high total crack length values for FM 7 for all strains. FM 7 has both the highest hafnium (3%) and carbon (500 ppm) content of all filler metals tested.

Note also the low crack length values of FM 4 (Ta-4W-1Hf) and FM 5 (Ta-4W-2Hf). Of the eight filler metals tested, these two were the lowest in alloying additions and in matrix strength. The difference between the total crack lengths of FM 4 and FM 5 is relatively small at the 2% and 4% strain levels. This is significant since FM 5 has twice the amount of hafnium in FM 4. It could be postulated that the hafnium concentration (as long as it is 2% or lower) is not as critical as the total amount of alloying additions in causing cracking.

Further combining the Varestraint data by adding the data at various strain levels for each of the filler metals and then ranking the filler metals according to the total crack length results in Table 8. The eight filler metals are ranked from worst, FM 7 (Ta-4W-3Hf-0.05C), with the most cracks, to the best, FM 4 (Ta-4W-1Hf), with the least amount of cracking.

From the Varestraint results, the eight filler metal compositions can be placed into four general groups. Both FM 4 and 5 have about the same total crack lengths, likewise for FM 1, 2, and 3 and FM 6 and 8. FM 7 is in a separate class with a very high total crack length. In support of the Varestraint groupings similar results would be arrived at based on alloying additions. FM 4 and 5 have relatively low tungsten and hafnium concentrations while FM 1, 2, and 3 have relatively high tungsten additions. FM 6 and 8 are high in both tungsten and hafnium-rhenium levels. FM 7 with its very high hafnium and carbon levels is in yet another group.

Table 8. Ranking of Filler Metals According to Results of
Varestraint Tests.

Filler Material Ranking (Cracking Sensitivity)		Total Crack Lengths Obtained From 2%, 3%, and 4% Varestraint Data	
		meters $\times 10^3$	mils (in $\times 10^3$)
Worst ↓ ↓ ↓ ↓ ↓ ↓ ↓ Best	7	157.7	6210
	6	73.4	2889
	8	62.1	2440
	1	38.0*	1495*
	3	44.9	1768
	2	38.0	1497
	5	21.1	830
	4	13.9	548

* Incomplete counting - numbers should be higher

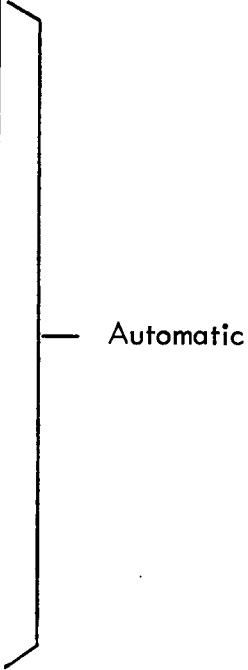
The Varestraint test did predict that all of the alloys tested were crack sensitive, some more than others. In addition, the results of the Varestraint testing provided a direct correlation of the effect of superimposed strain with defects observed metallographically in plate welds of similar composition. As shown in a previous program⁽⁵⁾ and again in the present program, the correlation between plate welding behavior and Varestraint results is excellent. These results provide the basis for possible wholesale substitution of Varestraint testing for the more expensive butt weld procedures in future testing. Used in such a way, Varestraint testing would provide a relatively inexpensive means of material qualification as a hardware specification requirement.

4.3 PLATE WELDMENT STUDIES

In this program a total of 29 GTA plate welds were prepared and evaluated. Table 9 lists each of these welds along with pertinent information. The first thirteen welds were made and metallographically examined to determine if filler metal compositional variations alone would eliminate underbead cracking in the single "V" multipass welds. The four filler metal compositions chosen from the Varestraint data and the five base line compositions used to prepare these welds are given below.

<u>FM No.</u>	<u>Nominal Composition (w/o)</u>
3	Ta-6W-1.5Hf
4	Ta-4W-1Hf
5	Ta-4W-2Hf
8	Ta-6W-0.8Re-1Hf-0.025C
9	Ta-unalloyed
10	Ta-4W
11	Ta-10W
12	Ta-0.5Hf
13	Ta-2Hf

Table 9. Plate Weldment Records

Ident. No.	FM	Joint Design	No. of Passes (Excluding Root)	Comments
1	3	Single "V"	16 - 10 IPM	
2	3	Single "V"	16 - 10 IPM	
3	4	Single "V"	16 - 10 IPM	
4	4	Single "V"	16 - 10 IPM	
5	5	Single "V"	17 - 10 IPM	
6	5	Single "V"	16 - 10 IMP	
7	8	Single "V"	16 - 10 IPM	
8	8	Single "V"	15 - 10 IPM	
9	9	Single "V"	16 - 10 IPM	
10	10	Single "V"	17 - 10 IPM	
11	11	Single "V"	14 - 10 IPM	
12	12	Single "V"	14 - 10 IPM	
13	13	Single "V"	13 - 10 IPM	
14	9	Single "V" Gap	2 manual	No land (Butt)
15	9	Single "V"	15 - 10 IPM	Duplicate of No. 9; Automatic
16	12	Single "V" Gap	4 manual	No land (Butt)
17	T-111	Single "V" Gap	2 manual	No land (Butt)
18	10	Single "V" Gap	3 manual	No land (Butt)
19	4	Single "V"	3 manual	No land (Butt)
20	4	Double "V"	12 manual	
21	4	Double "V"	4 manual	
22	10	Double "V"	12 - 10 IPM	Automatic
23	10	Double "V" Gap	6 manual	
24	10	Single "U" Gap	5 manual	No restraint
25	4	Double "V" Gap	4 manual	No land
26	4	Single "V" Gap	6 manual	No between pass cooldown
27	8	Single "V" Gap	4 manual	No between pass cooldown
28	4	Single "U" Gap	4 manual	Third pass remelted four times
29	T-111	Double "V" Gap	4 manual	No land

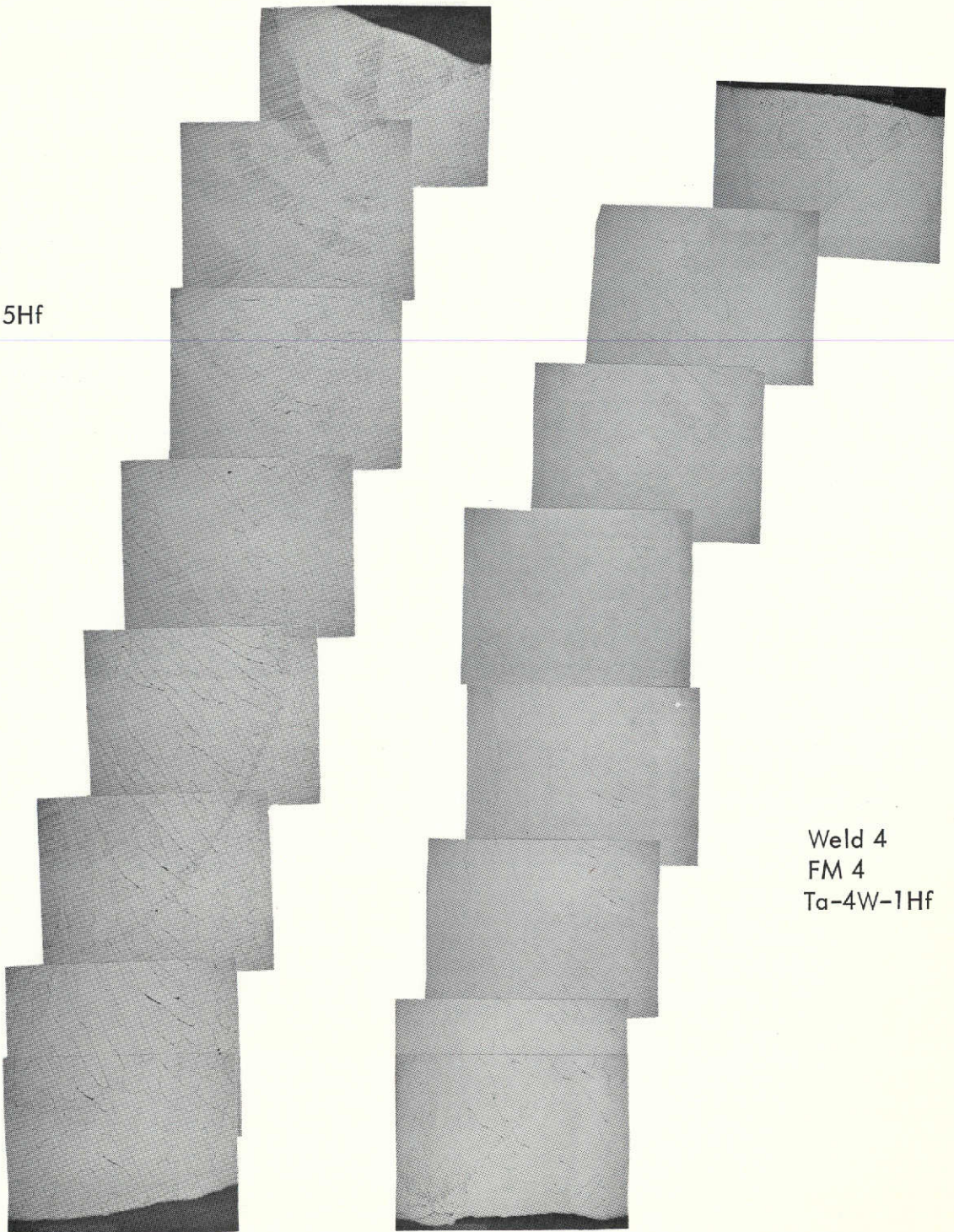
Two welds were made using each of FM 3, 4, 5, and 8 while one weld was made using each of FM 9, 10, 11, 12, and 13.

Evaluation for weld quality was accomplished by means of detailed metallographic examination of each weld joint. None of the initial thirteen weldments were totally crack free. Typical microstructures of the welds are shown in Figures 16 through 20. In all but the weld using FM 9 (pure Ta) the cracks are relatively small and do not extend over the full length of the grain boundary. The cracks in weldments 9 and 15 (FM 9) were the most severe noted and were present in both the weld metal and the heat affected zone. FM 9 (pure Ta) was expected to produce the best weld based on crack elimination but in fact produced the worst. The observed cracking is considered the result of the low mechanical strength of the filler metal and the resulting large amount of localized upsetting at weld root. The large amount of weld root deformation critically stressed the immediately adjacent structure (HAZ) resulting in extensive grain boundary cracking.

Based on the amount of underbead cracking, the welds prepared with FM 4 (Ta-4W-1Hf), FM 10 (Ta-4W), and FM 12 (Ta-0.5Hf) were the best of the series. Each of these filler metals are low in both total alloying additions and in hafnium. In general, all of the welds, except those prepared with FM 9 (pure Ta), had basically sound structures, although scattered small cracks were present at the grain boundaries of all welds. Some of the "cracks" observed on Figures 16-20 appear exaggerated in magnitude due to etching effects during metallographic preparation.

Based on the results of the first 13 welds, FM 4 (Ta-4W-1Hf) and FM 10 (Ta-4W) were selected for use in the study of procedural and joint design effects. FM 4 was shown by the Vareststraint data to be the best of the original eight filler metals tried. FM 10 was chosen along with FM 4 because it is the same chemistry except it contains no hafnium and thus provides basic information from which the effect of hafnium on the weld structures could be derived.

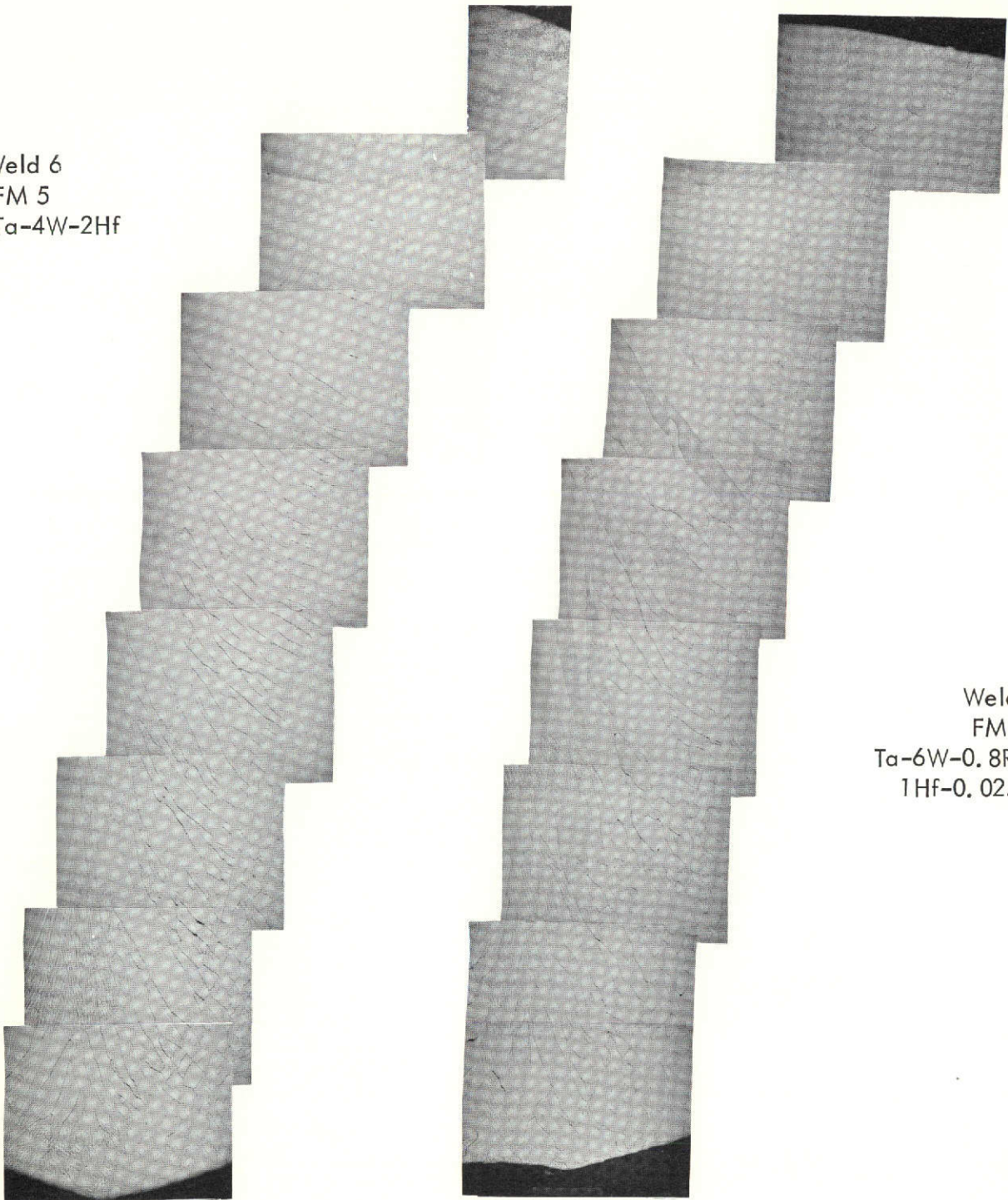
Weld 2
FM 3
Ta-6W-1.5Hf



Weld 4
FM 4
Ta-4W-1Hf

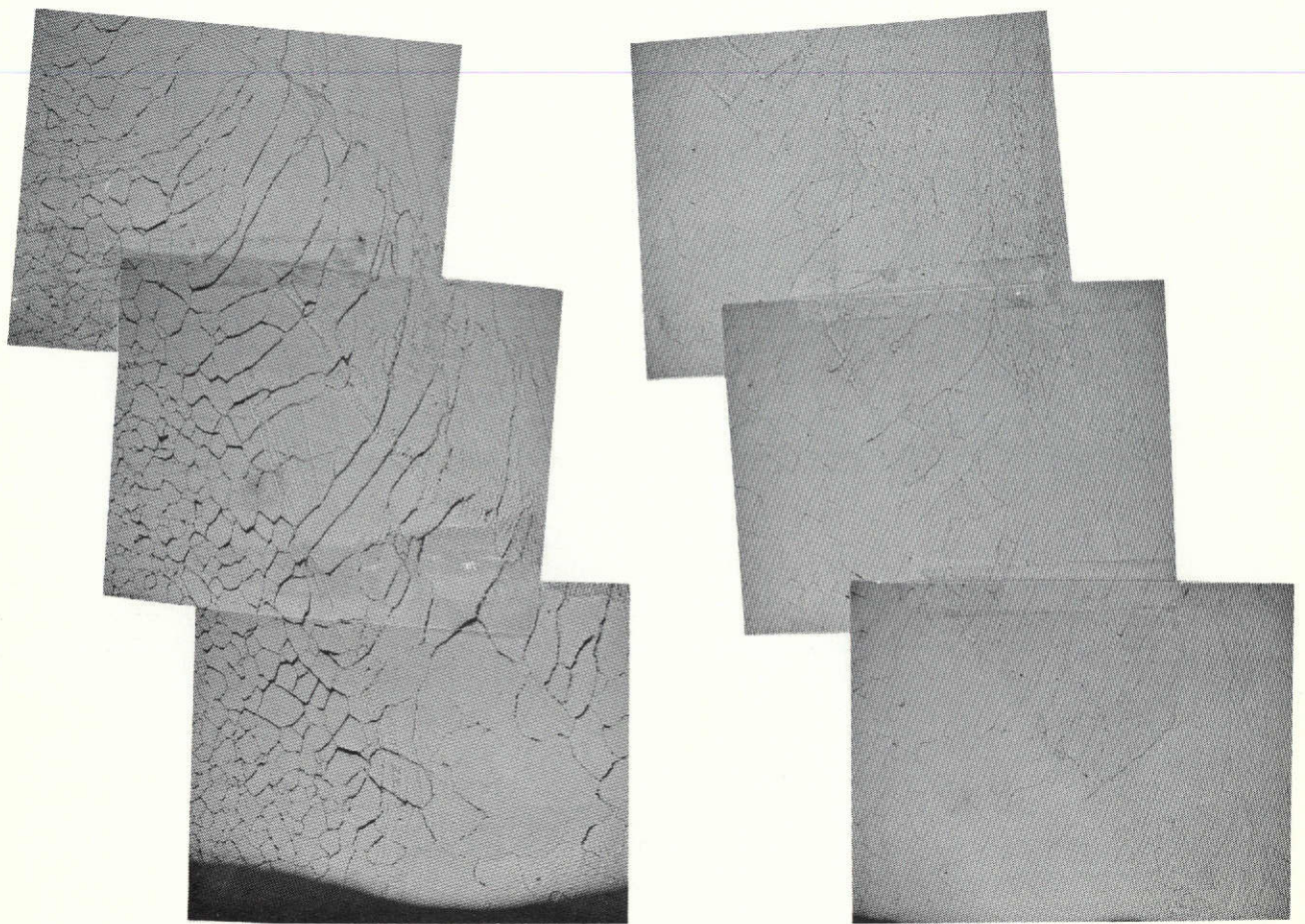
Figure 16. Microstructures of Single "V" Welds 2 and 4

Weld 6
FM 5
Ta-4W-2Hf



Weld 8
FM 8
Ta-6W-0.8Re-
1Hf-0.025C

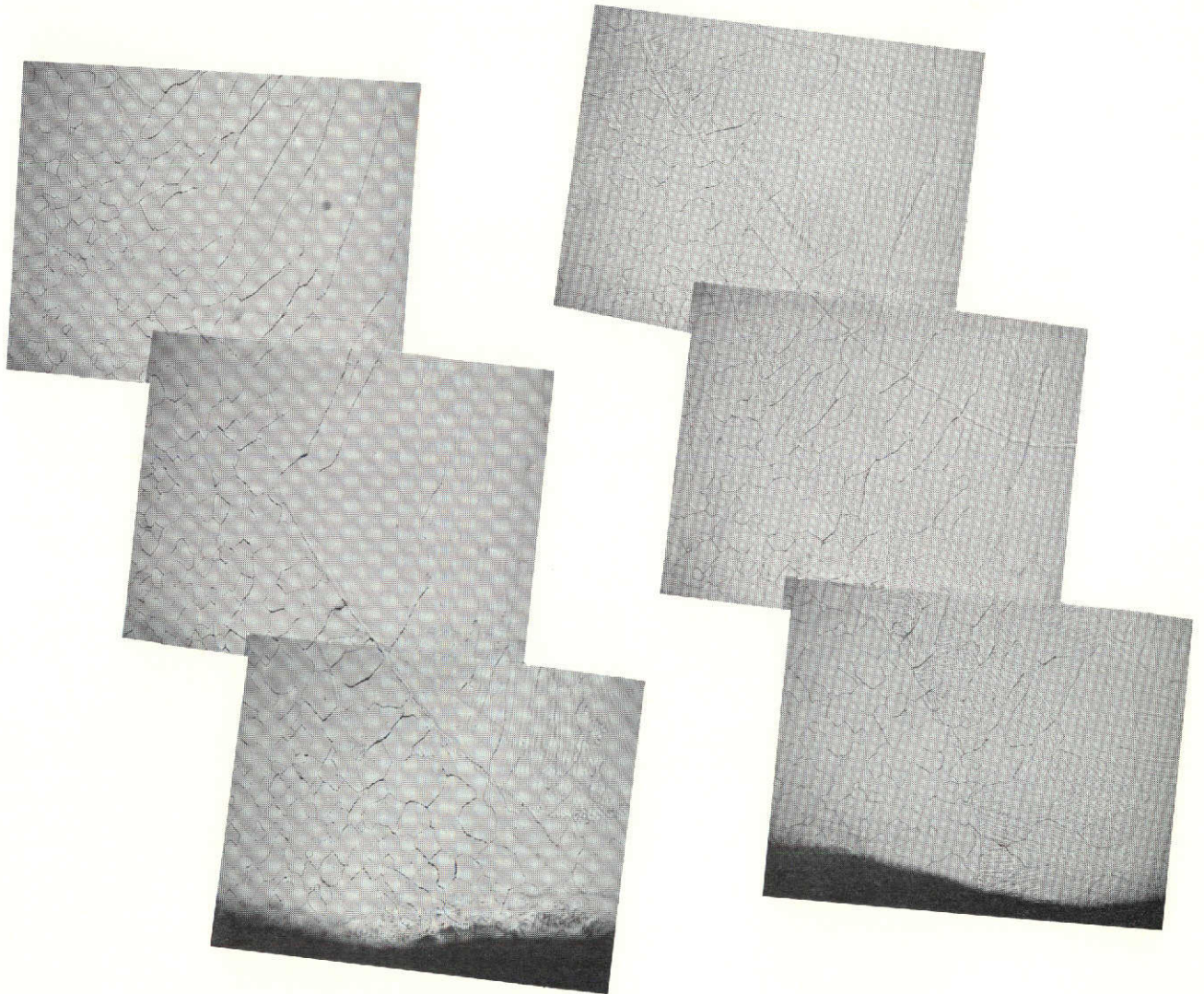
Figure 17. Microstructures of Single "V" Welds 6 and 8.



Weld 9
FM 9
Pure Tantalum

Weld 10
FM 10
Ta-4W

Figure 18. Microstructures of Single "V" Welds 9 and 10



Weld 11
FM 11
Ta-10W

Weld 12
FM 12
Ta-0.5 Hf

Figure 19. Microstructures of Single "V" Welds 11 and 12

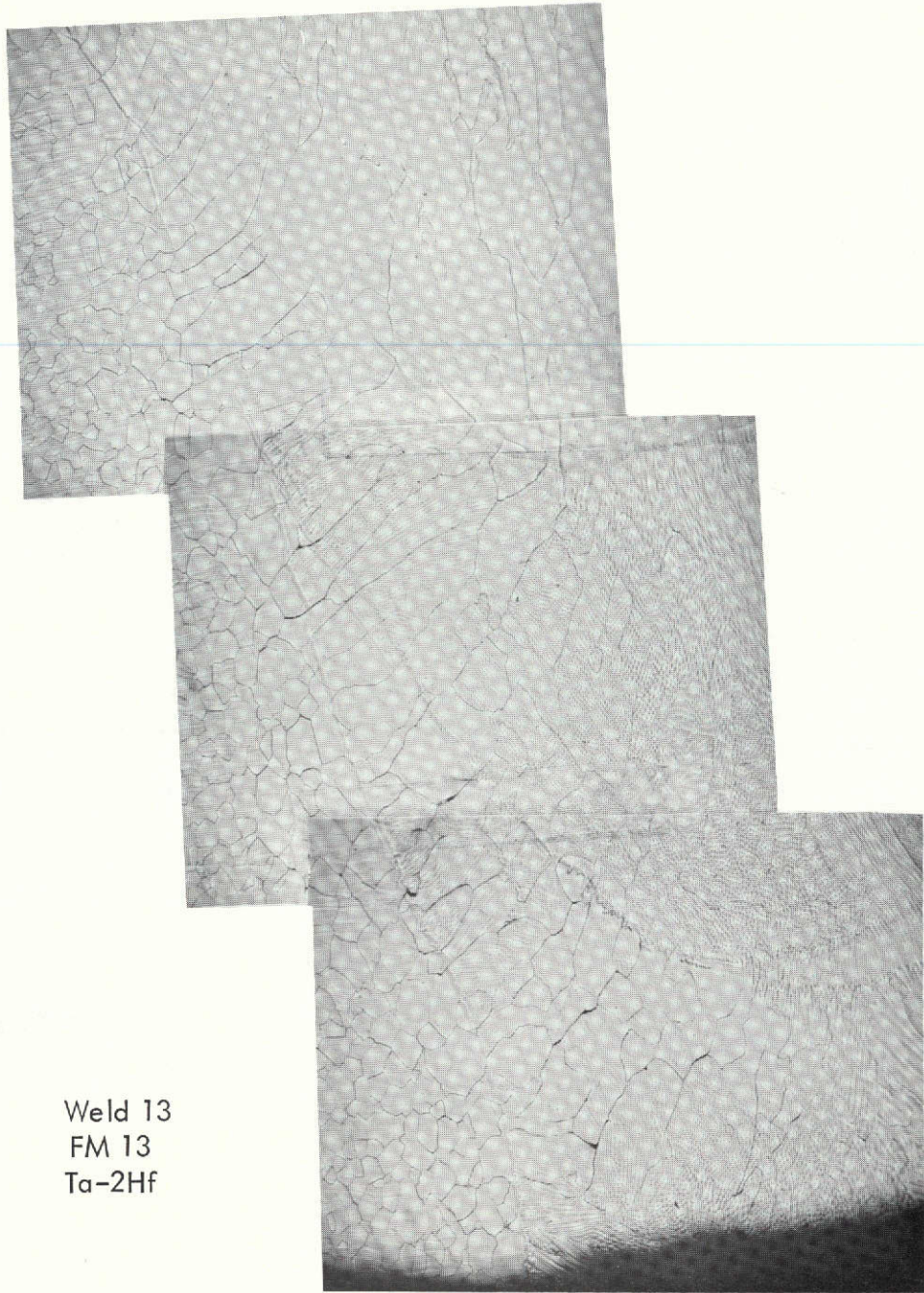


Figure 20. Microstructure of Single "V" Weld 13

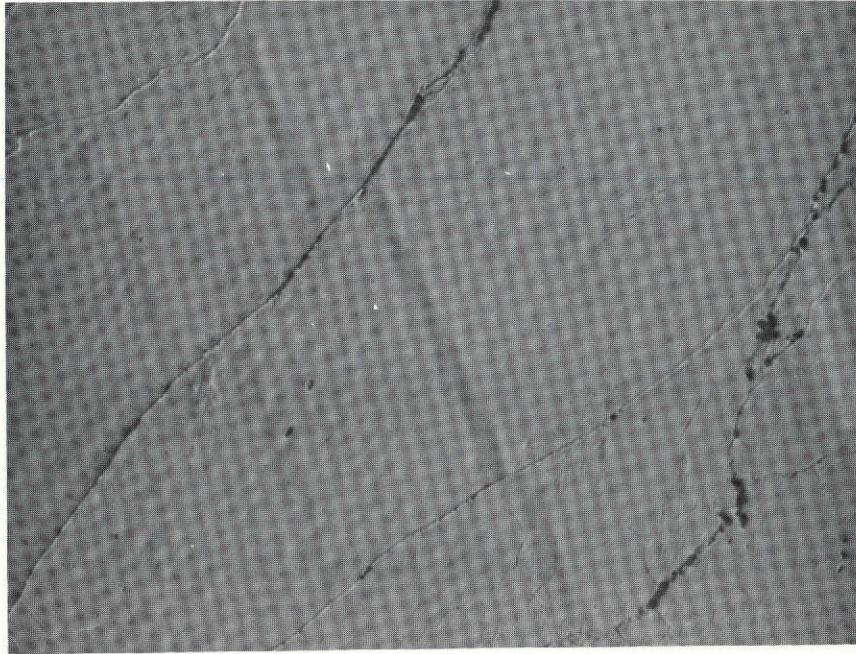
The basic factor underlying the weld bead cracking is that the stress/strain imposed upon the underbead structure during subsequent thermal cycles produces significant shear along the grain boundary. This shear phenomenon can be seen in the weldment microstructures. Solute lines representing boundary areas between molten and solid filler metal are continuous across adjacent grains. These artifacts are readily seen in the weld structures shown in Figures 16 through 20. Close examination of the solute lines in the underbead area where cracking occurs indicates that these lines are often discontinuous at the grain boundaries. A photomicrograph of such a structure is presented in Figure 21. The solute lines are the thin shaded areas running nearly perpendicular to the grain boundary. The fact that these lines are discontinuous at the grain boundary and straight within the grain indicates that the majority of strain occurring within the weld is accommodated by grain boundary sliding.

Large amounts of grain boundary sliding can result in either complete grain boundary separation as shown in Figure 22, or the boundary may remain unchanged as was seen in Figure 21. Grain boundary sliding is present to some degree in all the weld structures, but cracking usually occurs only in the areas where hafnium is present, such as in the root fusion area and at the weld metal HAZ interface. Therefore, it is postulated that hafnium adversely affects the grain boundary properties resulting in crack formation.

4.4 PROCEDURAL AND DESIGN CHANGES

None of the filler metals were capable of producing totally crack-free welds using standard multipass welding practices. This implied a solution based solely on metallurgical variations was not possible. Hence, variations in weld procedure were tried. The major procedural variation considered was to alter the number of weld passes used to produce the weldment.

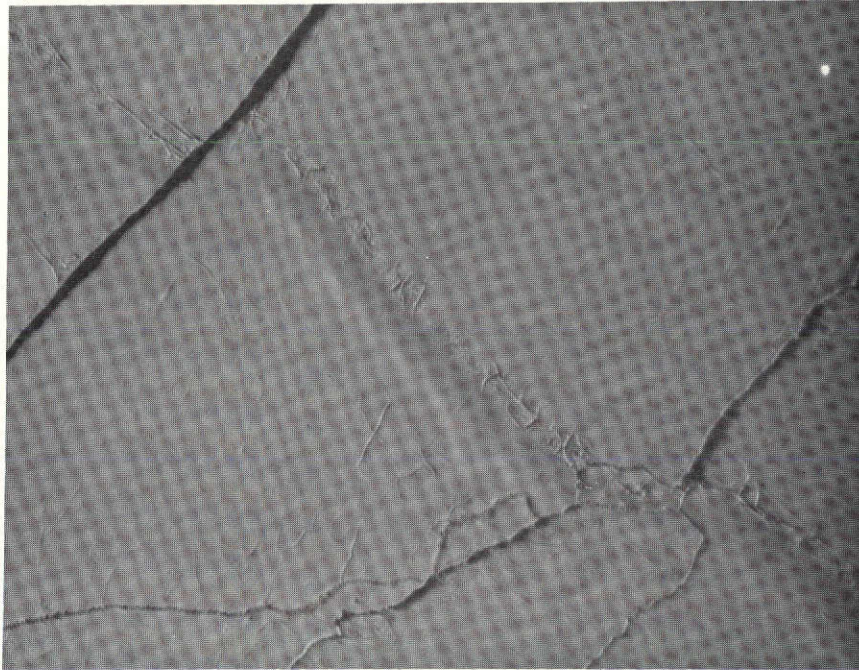
Weld 14 was made with FM 9 (Ta) using the single "V" groove joint design but with the lands ground off. Only two filler passes were used to complete the weld. No root fusion pass was used, and the resultant weld had a poor root structure and incomplete weld penetration.



24,187

400 X

Figure 21. Example of Grain Boundary Sliding in Multipass
GTA Plate Weldment



24, 187

700 X

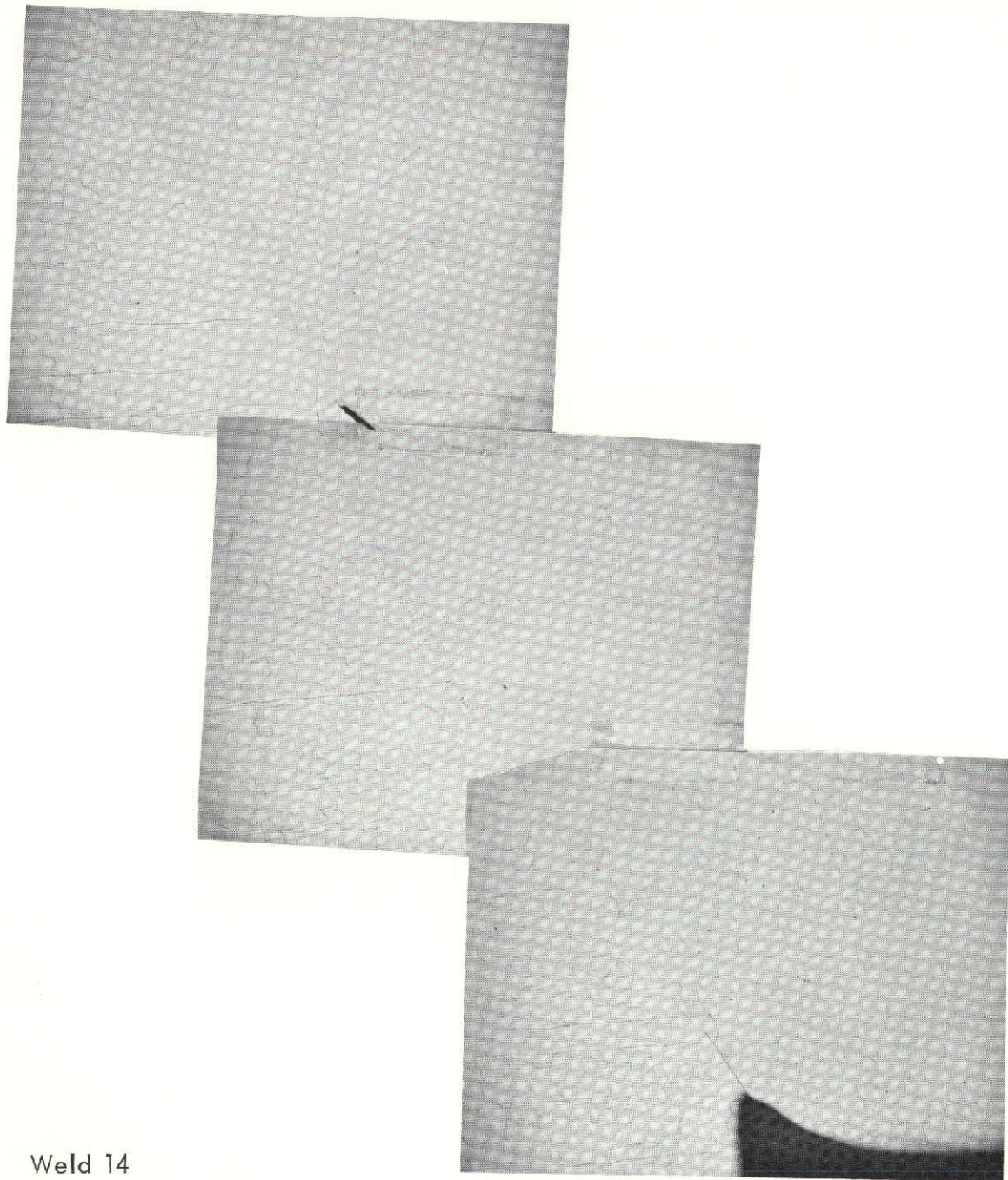
Figure 22. Example of Grain Boundary Cracking in Multipass
GTA Plate Weldment

However, there were no underbead cracks in the weld, Figure 23. Compare this to the very heavily cracked single "V" weld 9 made using standard multipass methods, Figure 18. Note the incompletely welded area about two-thirds of the way up the photomicrograph. The chances for this type of problem are much greater in a minimum-pass weldment but are not considered as critical problems since they can be avoided with experience. In subsequent welds the problems of incomplete weld penetration and poor root areas were solved by gapping the weld blanks by 0.15 cm (0.06 inch) and making a root pass with filler metal.

The rapid fill (2 to 4 pass) technique was used to prepare four additional plate welds. These are numbered 16, 17, 18, and 19 on Table 9 and were identical, except for weld 17 which used T-111 as the filler metal, to welds produced in the initial series of plate welds. Cracking again occurred in welds 16, 17, and 19 but was less severe than observed in corresponding welds made using standard > 4-pass techniques. Weld 18, made with FM 10, was crack free as seen in Figure 24.

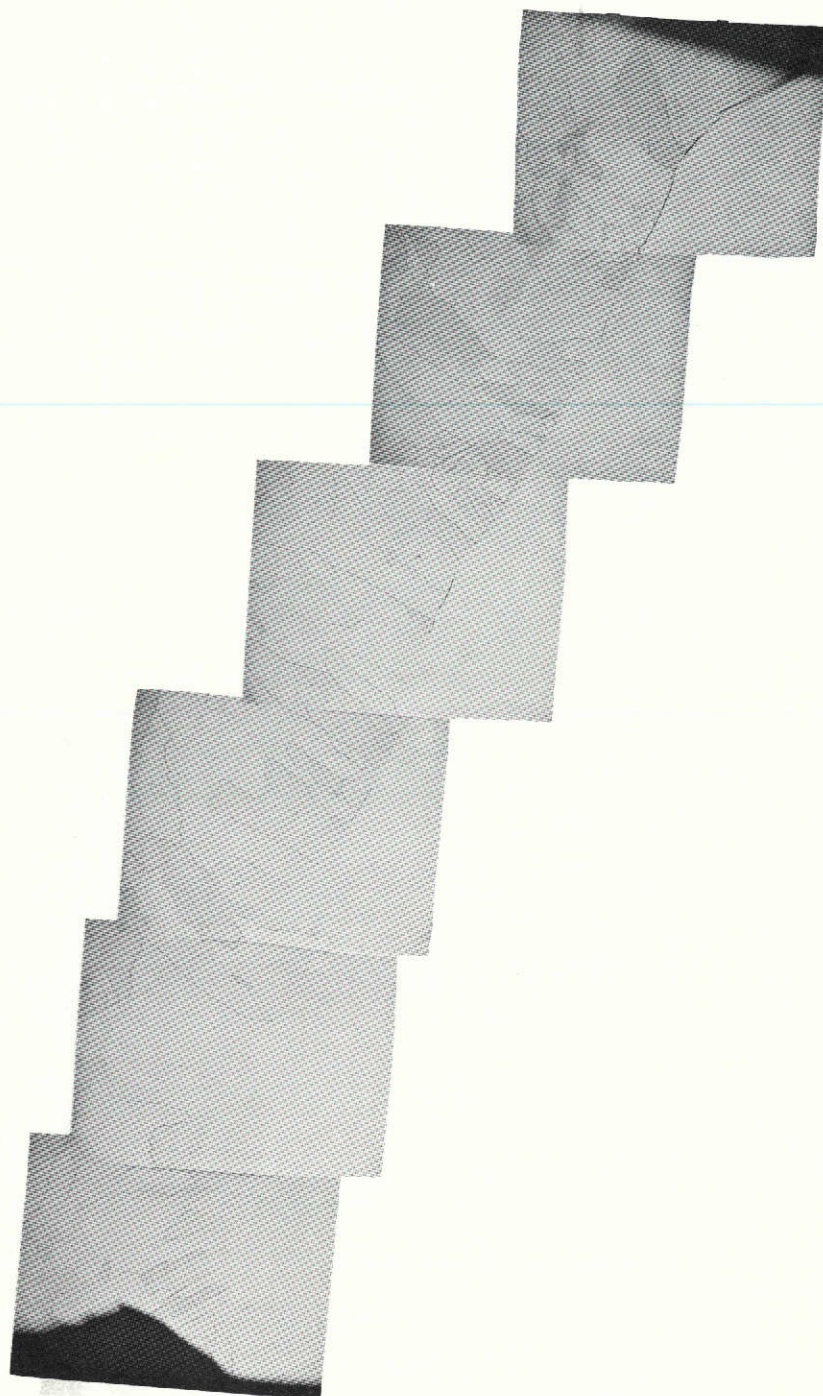
It is significant to note that both weld 14, prepared with FM 9 (unalloyed Ta), and weld 18, prepared with FM 10 (Ta-4W), were completely free of underbead cracking. Hence, crack-free single "V" GTA welds can be made in T-111 plate so long as the filler metal does not contain hafnium and a minimum-pass welding procedure is used. The latter condition probably derives from the fact that this procedure minimizes hafnium pickup from the T-111 base metal.

In an effort to minimize the severity of thermal cycling during welding, welds 26 and 27 were prepared without the use of an interpass cooldown period as is normally used. These welds used the single "V" groove design and were made using the minimum-pass procedure. When a weld pass was complete, the next pass was started as soon as possible. Thermocouples were attached to the weld blanks in order to monitor the thermal cycles. The cooldown of the specimen was so rapid after the arc passed that temperatures above 1000°C were present



Weld 14
FM 9
Pure Tantalum

Figure 23. Microstructure of Single "V" Weld 14



Weld 18
FM 10
Ta-4W

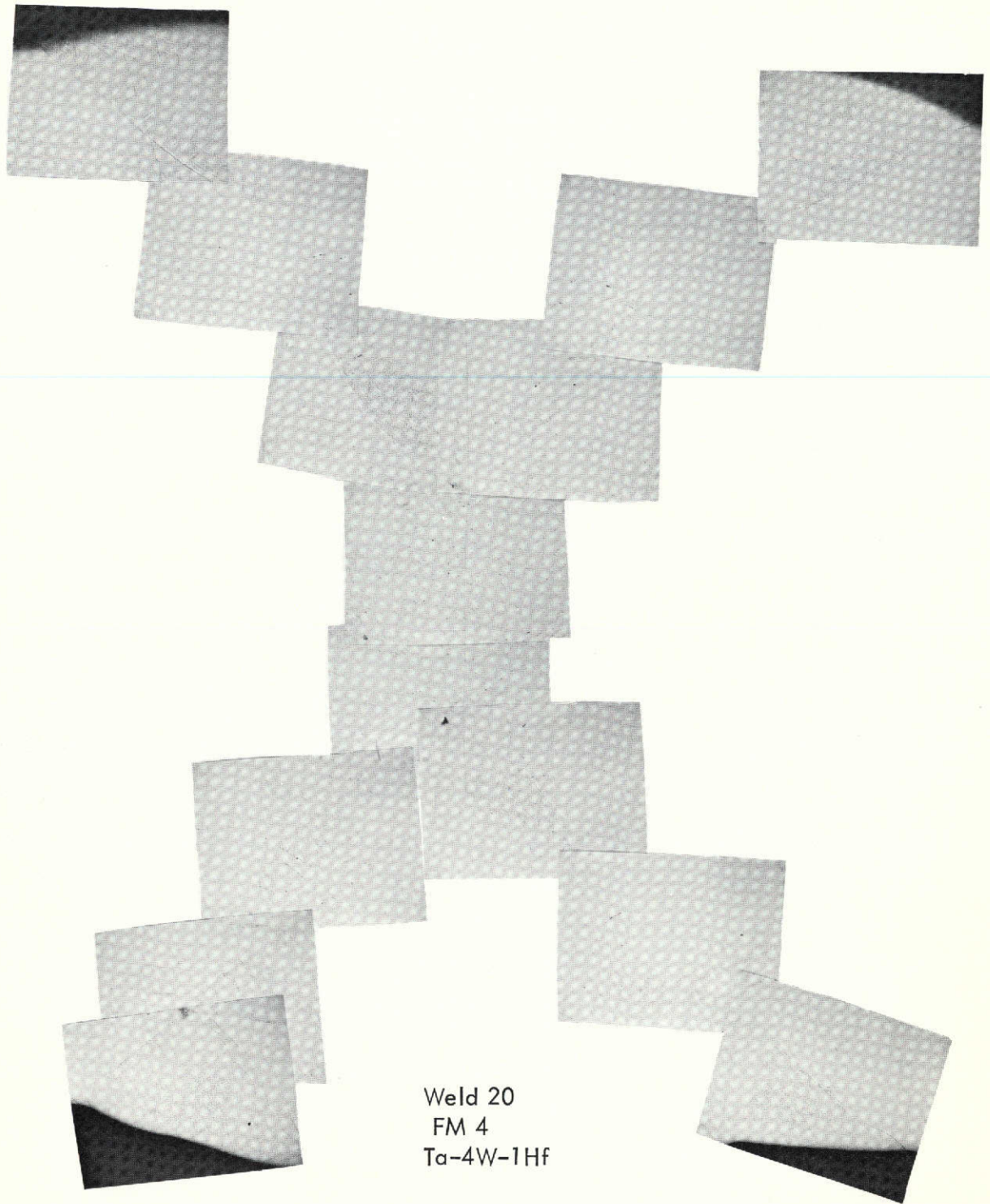
Figure 24. Microstructure of Single "V" Weld 18

for only about 4 seconds after the peak temperature was reached and the weld heated from 1000°C to the maximum temperature in less than 1 second as the arc approached. From the information recorded it was assumed that the specimen's cooling rate was so rapid that temperatures above 600°C could not be maintained for prolonged periods, greater than 10 seconds, and that unless a preheat fixture capable of maintaining temperatures in excess of 1000°C were available, the thermal cycling inherent in the weld procedure, and a major contributor to underbead cracking, could not be significantly altered by external heating.

Attempts to eliminate or reduce the problem of underbead cracking via weld design changes were limited to the use of modified single "U" groove (Figure 8) and double "V" groove (Figure 9) configurations. The single "U" groove design proved no better than the single "V" geometry since the same unbalanced stress cycling occurs during successive weld passes.

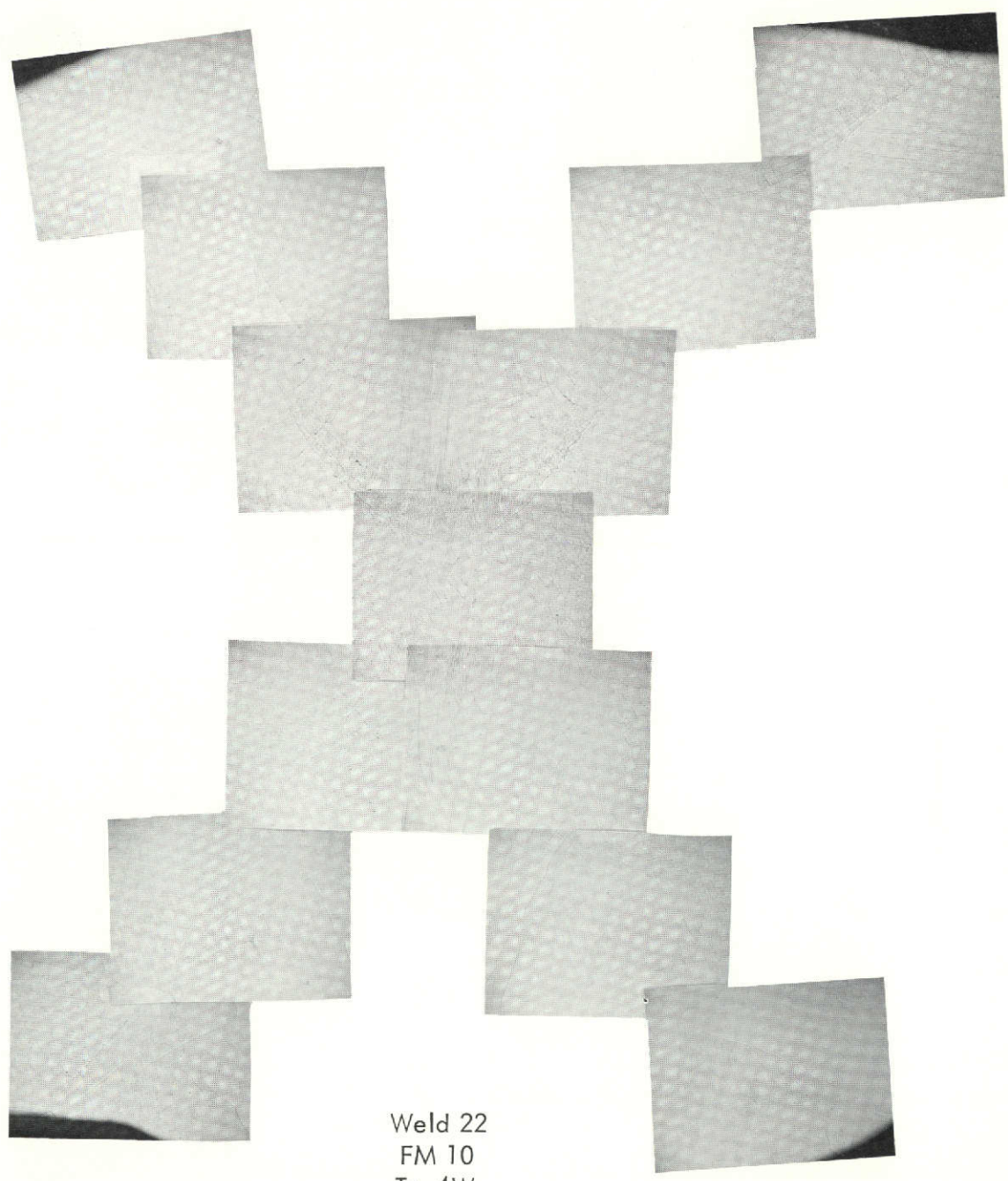
Use of the double "V" geometry produced much better results. Welds 20 through 23, 25, and 29 were prepared in this way. Examples of the weld microstructures are presented in Figures 25, 26, and 27. Even when T-111 was used as the filler metal (weld 29, Figure 27) the amount of underbead cracking which could be detected metallographically was insignificant. As pointed out previously, however, this joint design is not, in general, practical for many applications requiring heavy plate welding of T-111.

In general, the double "V" joint produces excellent welds regardless of filler metal composition although the best joints were made using FM 10 (Ta-4W) and a minimum number of passes. Similarly, the quality of the single "V" joint appears to be much more sensitive to weld procedures than to the filler metal used. Using FM 9 (unalloyed Ta) and 12 passes, the worst case of weldment cracking was observed; however, using the same filler metal but with 2 passes, the weld produced was completely crack free.



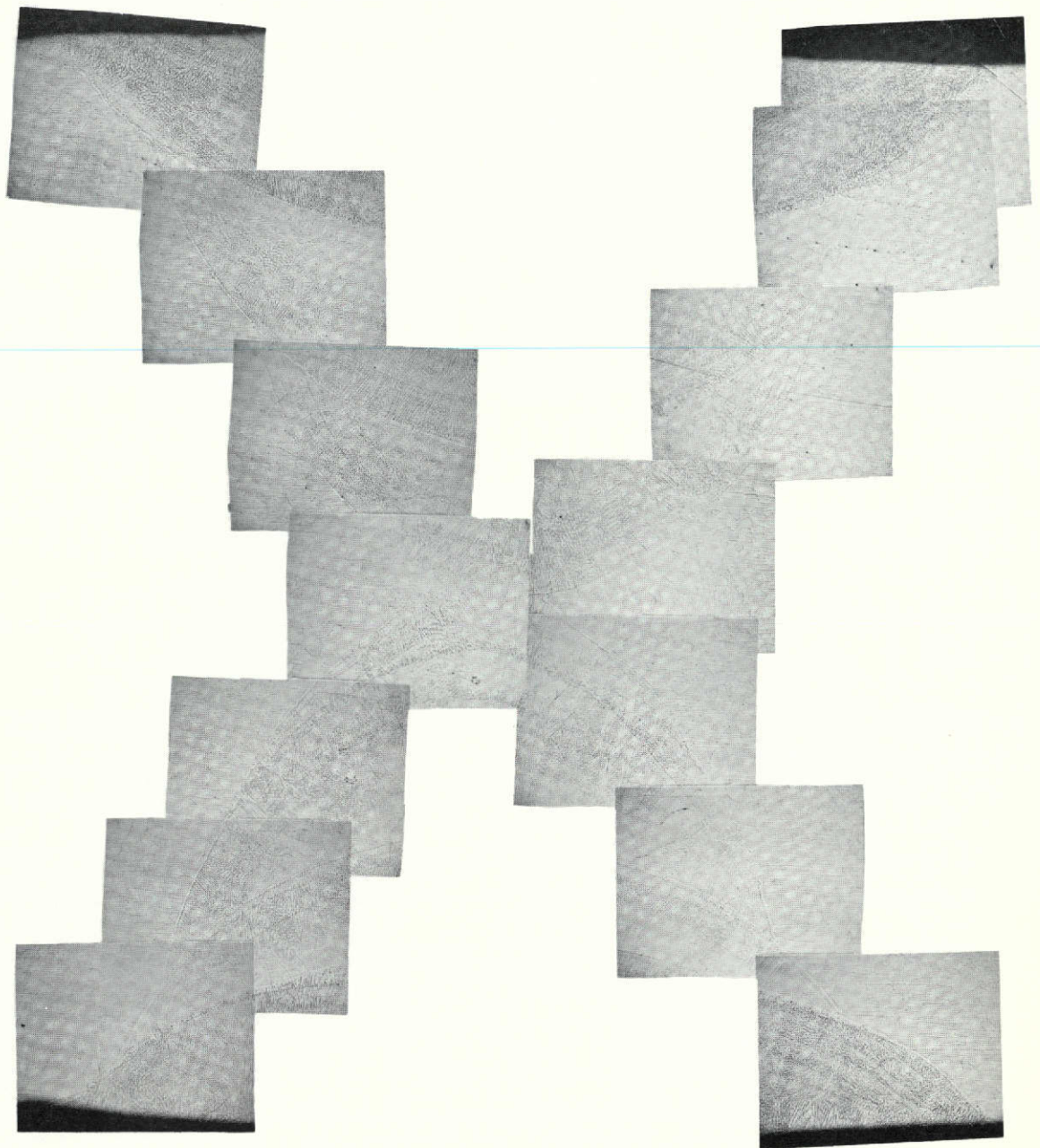
Weld 20
FM 4
Ta-4W-1Hf

Figure 25. Microstructure of Double "V" Weld 20



Weld 22
FM 10
Ta-4W

Figure 26. Microstructure of Double "V" Weld 22



Weld 29
T-111 Filler Metal

Figure 27. Microstructure of Double "V" Weld 29

4.5 TENSILE TESTS

In addition to the optical metallographic evaluation of the plate welds, the room temperature tensile properties were determined for each of the filler metal compositions and 1649°C (3000°F) tensile properties were determined for welds 2, 4, 6, and 8. Specimens were machined from the plate welds to permit transverse tensile testing, i. e., the longitudinal weld axis was normal to the longitudinal axis of the round bar tensile specimens. The results of these tests are presented in Table 10.

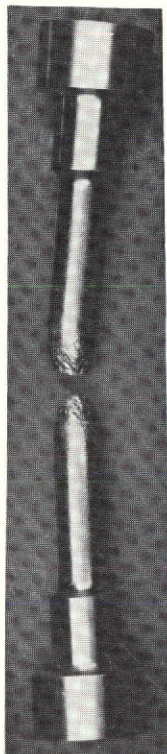
Three as-tested specimens are shown in Figure 28. The specimens machined from weld 7 and weld 20 are not typical in that failure occurred in the parent metal, away from the weld. The results of these tests and observations made on the tested specimens are summarized below:

- At room temperature and 1649°C (3000°F) the presence of underbead cracks in plate weldments does not measurably affect joint strength.
- Although failures generally occur in the weld metal, this is undoubtedly strongly influenced by the large and unfavorably oriented grain structure of the weldment.
- Ductility, as reflected by percent elongation at failure, is noticeably less for the plate weld specimens than for T-111 base metal. As for the preceding observation, the large grain size of the weldment would have a significant influence here and make it rather difficult to separate and identify any portion of the reduced ductility as being due to the presence of underbead cracks.
- From the limited number of comparisons available, double "V" joint welds appear stronger than similarly prepared single "V" welds.

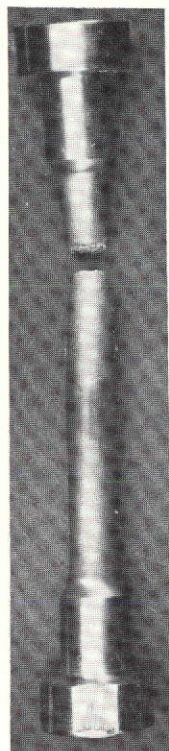
Table 10. Tensile Test Results

FM Ident. No. No.	Nominal Composition (w/o)	Test Temperature °C (°F)	UTS		0.2% YS		Total Elong. %	RA %
			10^7N/m^2	ksi	10^7N/m^2	ksi		
3 1	Ta-6W-1.5Hf	RT (-)	58.0	84.1	50.4	73.1	7.84	14.8
3 2	Ta-6W-1.5Hf	1649 (3000)	12.2	17.7	11.4	16.5	1.17	1.5
4 3	Ta-4W-1Hf	RT (-)	54.7	79.3	48.3	70.1	4.62	6.1
4 4	Ta-4W-1Hf	1649 (3000)	12.1	17.5	11.5	16.7	1.84	5.2
5 5	Ta-4W-2Hf	RT (-)	52.9	76.7	44.1	63.9	6.50	32.2
5 6	Ta-4W-2Hf	1649 (3000)	12.5	18.1	11.7	17.0	3.60	5.0
8* 7	Ta-6W-1Re- 0.8Hf-0.025C	RT (-)	62.7	90.9	51.2	74.2	17.30	34.6
8 8	"	1649 (3000)	12.5	18.1	11.6	16.8	7.88	2.0
9 9	Ta-unalloyed	RT (-)	43.4	62.9	37.9	55.0	9.00	22.7
10 10	Ta-4W	RT (-)	47.4	68.8	33.5	48.6	9.00	28.0
11 11	Ta-10W	RT (-)	56.1	81.3	50.4	73.1	2.84	8.2
12 12	Ta-0.5Hf	RT (-)	42.7	62.0	34.2	49.6	11.60	48.5
13 13	Ta-2Hf	RT (-)	49.0	71.1	41.2	59.8	10.32	32.2
9 14	Ta-unalloyed	RT (-)	45.4	63.9	36.0	52.2	7.31	34.6
9 15	Ta-unalloyed	RT (-)	40.7	59.0	31.6	45.8	11.5	55.3
12 16	Ta-0.5Hf	RT (-)	35.3	51.2	27.2	39.4	8.8	37.4
T-11 17	Ta-8W-2Hf	RT (-)	58.5	84.9	50.2	72.8	6.14	5.3
10 18	Ta-4W	RT (-)	39.7	57.6	33.0	47.8	9.01	36.2
4 19	Ta-4W-1Hf	RT (-)	50.8	73.7	48.3	70.1	0.9	6.3
4* 20	Ta-4W-1Hf	RT (-)	60.7	88.0	50.7	73.5	30.4	87.4
4 21	Ta-4W-1Hf	RT (-)	58.6	85.0	50.5	73.2	11.3	13.9
10 22	Ta-4W	RT (-)	60.5	87.7	50.5	73.2	22.0	41.3
10 23	Ta-4W	RT (-)	59.9	86.9	50.2	72.8	18.9	53.8

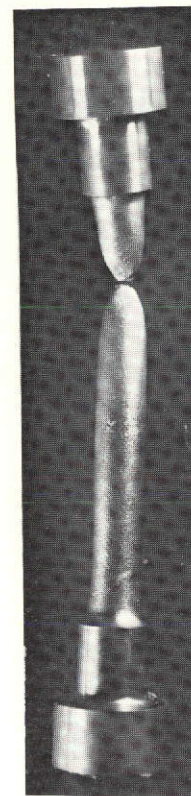
* Specimen failed outside of weld area



Weld 4
FM 4
Ta-4W-1Hf
Tested at 1649°C



Weld 7
FM 8
Ta-6W-0.8Re-1Hf-0.025C
Tested at RT



Weld 20
FM 4
Ta-4W-1Hf
Tested at RT

Figure 28. As-tested Tensile Specimens. Specimens Machined from Multipass GTA Plate Weldments.

- A general correlation between filler metal hardness and weld joint tensile strength was observed, Figure 29. The relationship implied by Figure 29 is a trend rather than a direct correlation since the as-welded hardness would be somewhat higher than the rolled/annealed hardness values used.

4.6 BEND TESTS

Prior to bend testing the surfaces of the test welds were inspected for weld defects using dye penetrant techniques. Cracking was not detected for any of the welds. Typical results are shown in Figure 30.

Bend specimens were prepared from welds 18 through 24. These welds had been made using either FM 4 (Ta-4W-1Hf) or FM 10 (Ta-4W). Bending was achieved by using a 1 t punch radius and bending the specimens 90° or until the punch contacted the specimen at a point other than at the punch tip. Welds 18, 19, and 24, which were single "V" welds, were tested in such a manner that the top surface of the weld was in tension. For welds 20-23, which were double "V" welds, the top and bottom surfaces are indistinguishable. The data obtained from these tests are presented in Table 11. The outer fiber stress and approximate outer fiber strain were determined from the following formulas:

$$\text{Stress} = \frac{1.5 WL}{BH^2} \qquad \text{Strain (\%)} = \frac{6HD^4}{W^2}$$

- W - Span length
- L - Load
- B - Specimen width
- H - Specimen thickness
- D - Deflection

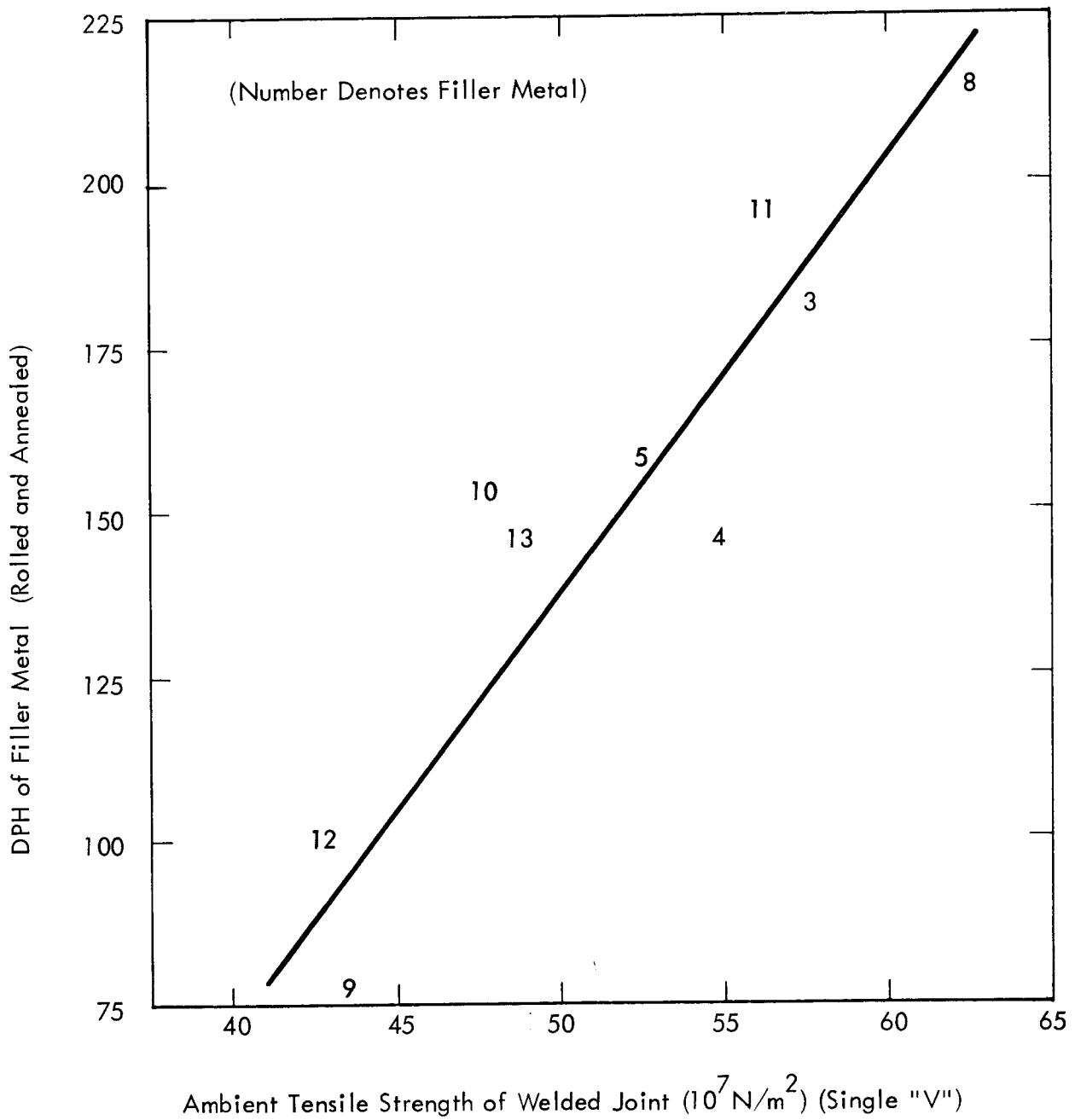
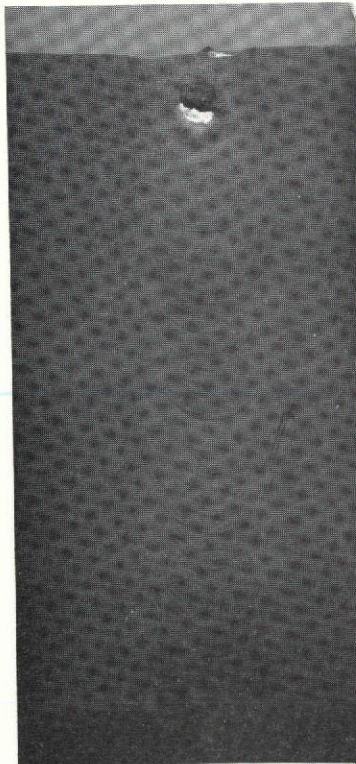
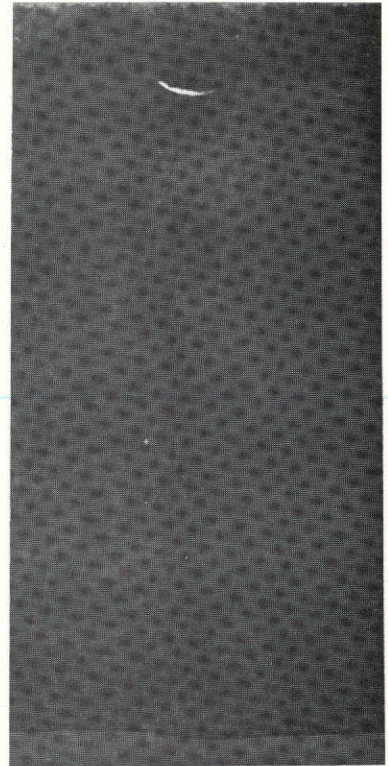


Figure 29. Relationship Between Filler Metal Hardness and Weld Strength at Ambient Temperature



TOP



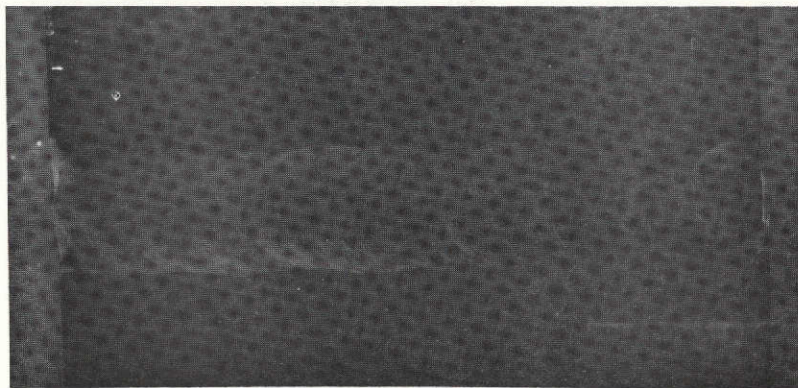
ROOT

Weld Number 19

FM 4

(Ta-4W-1Hf)

Single "V"



TOP
Weld 21

FM 4

Ta-4W-1Hf

Double "V"

Figure 30. Typical Results of Dye Penetrant Inspection of As-welded Butt Welds

Table 11. Results of Bend Tests on Welded Joints

Weld No.	Filler Metal No.	Joint Description	Final Stress		P. L. Stress **		Approx. Strain (%)
			(10^7N/M^2)	(ksi)	(10^7N/M^2)	(ksi)	
19	4	Single V 3 pass	127.8	185.4	63.2	91.7	31
20*	4	Double V 12 pass	132.2	191.7	89.9	130.4	40
21	4	Double V 4 pass	122.2	177.2	78.7	114.2	43
18	10	Single V 3 pass	111.1	161.1	58.0	84.1	39
22	10	Double V 12 pass	118.1	171.3	79.4	115.2	39
23	10	Double V 6 pass	111.0	161.0	66.9	97.1	35
24	10	Single U 5 pass	111.6	161.9	67.3	97.6	36

* Weld direction parallel to punch direction

** P. L. = proportional limit

Failure did not occur during any tests. The tests were stopped when the punch began loading on areas on its sides rather than its radius. The stress at the initiation of plastic deformation is reported in Table 11 as P. L. (for proportional limit).

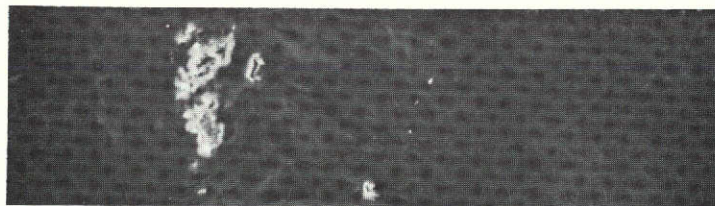
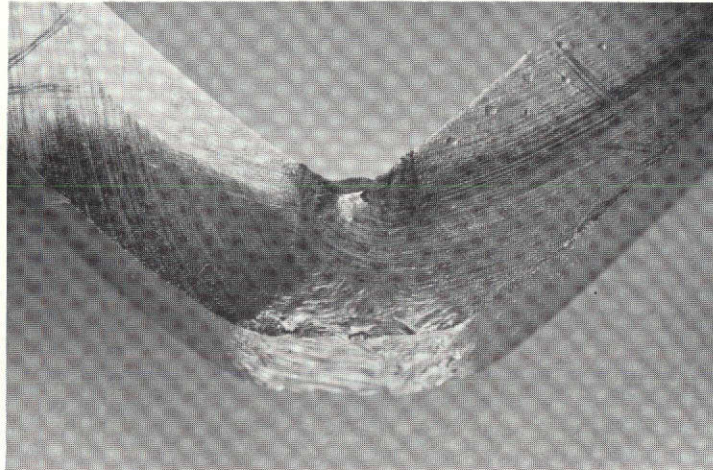
Following bend testing, the specimens were again inspected for defects with dye penetrant techniques. Figures 31 and 32 show both the bent specimen and the dye penetrant indications of welds 18 and 19. These results are typical showing one instance where significant cracking was detected on the outer surfaces and a comparatively crack-free bend specimen. One bend test, on weld 20, was performed on the specimen after rotating it 90° about its axis. In that orientation the punch moved in a direction parallel to the weld direction. No evidence of cracking was seen following bend testing.

Figures 33-35 show the results of metallographic examination of several specimens following bend testing. Figures 34 and 35 compare pre-test and post-test structures of welds 19 and 24, respectively. Both of these welds were made in the single "V" joint design and contained a small, but discernible, amount of underbead cracking as welded. The bend testing has resulted in the enlargement of the existing cracks and initiated others. However, while the cracks do enlarge during deformation, their presence does not seem to greatly alter the bend behavior of plate weldments containing them.

Figure 35 shows the post-test microstructure of a specimen prepared from a double "V" weld joint -- weld 23. There were no indications of cracking before testing, and none appeared following, despite the fact the outer fiber strain reached approximately 35% during testing.

4.7 MICROPROBE ANALYSIS

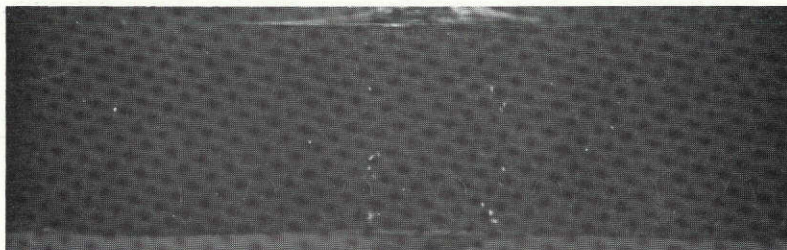
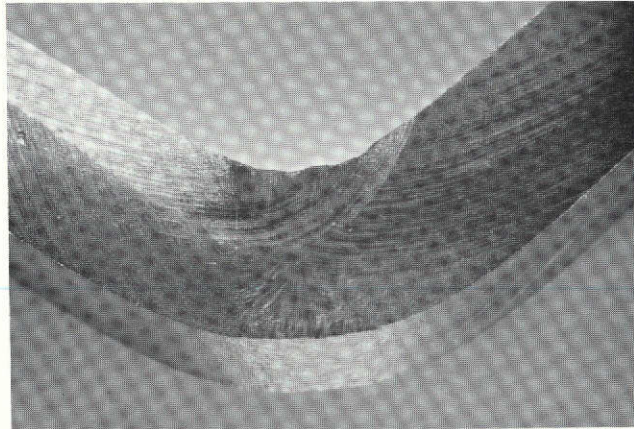
In an effort to determine the extent of solute segregation in the weldment, a specimen removed from weld 4 (FM 4, Ta-4W-1Hf) was analyzed for hafnium with an electron beam microprobe. The nominal hafnium concentrations in the T-111 base metal and the filler



Weld 18

FM 10 Ta-4W

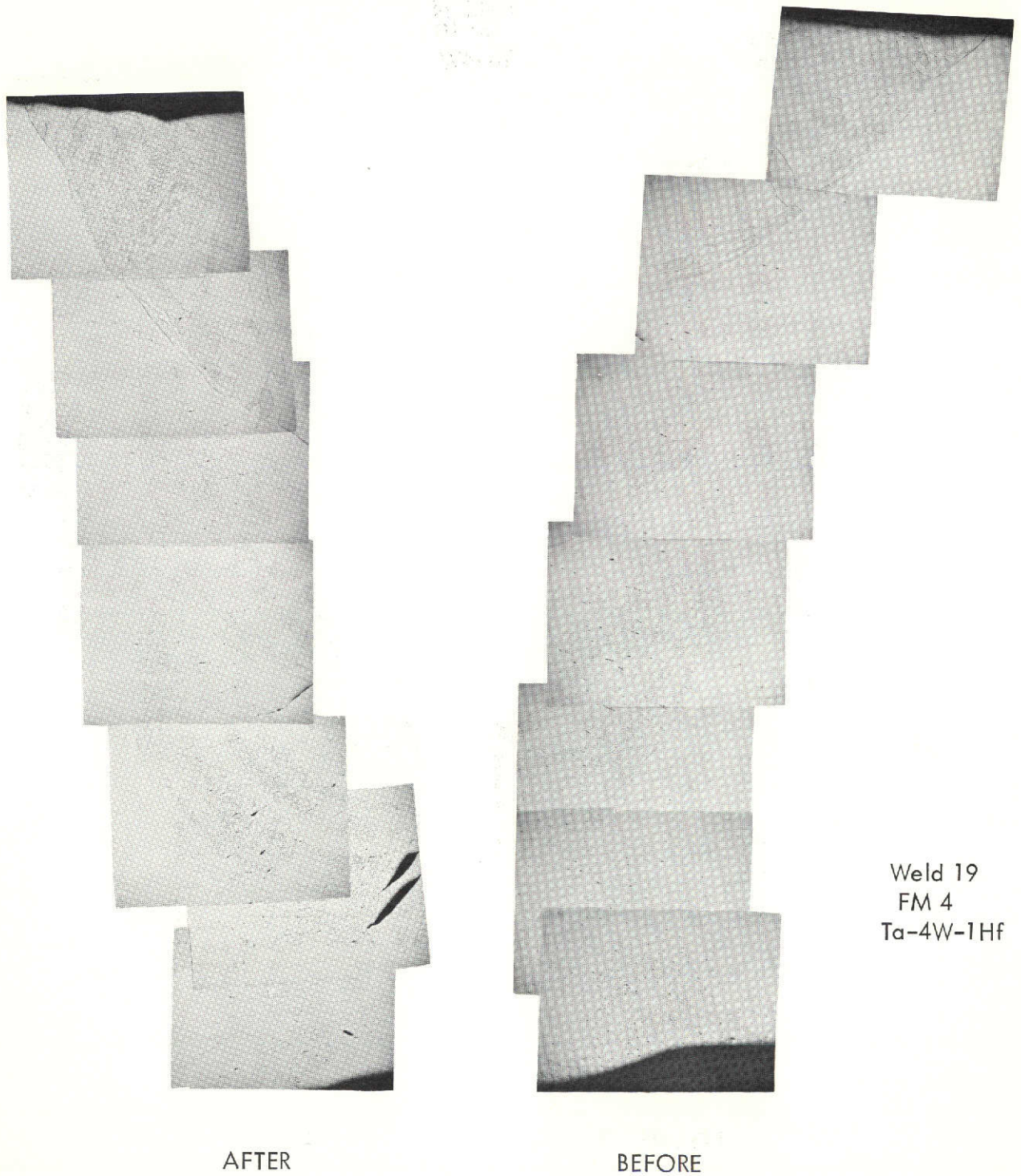
Figure 31. As-Bend Tested Plate Weld Specimen. Single "V"
Weld Tested with Top Face of Weldment in Tension



Weld 19

FM 4 Ta-4W-1Hf

Figure 32. As-Bend Tested Plate Weld Specimen. Single "V" Weld Tested with Top Face of Weldment in Tension



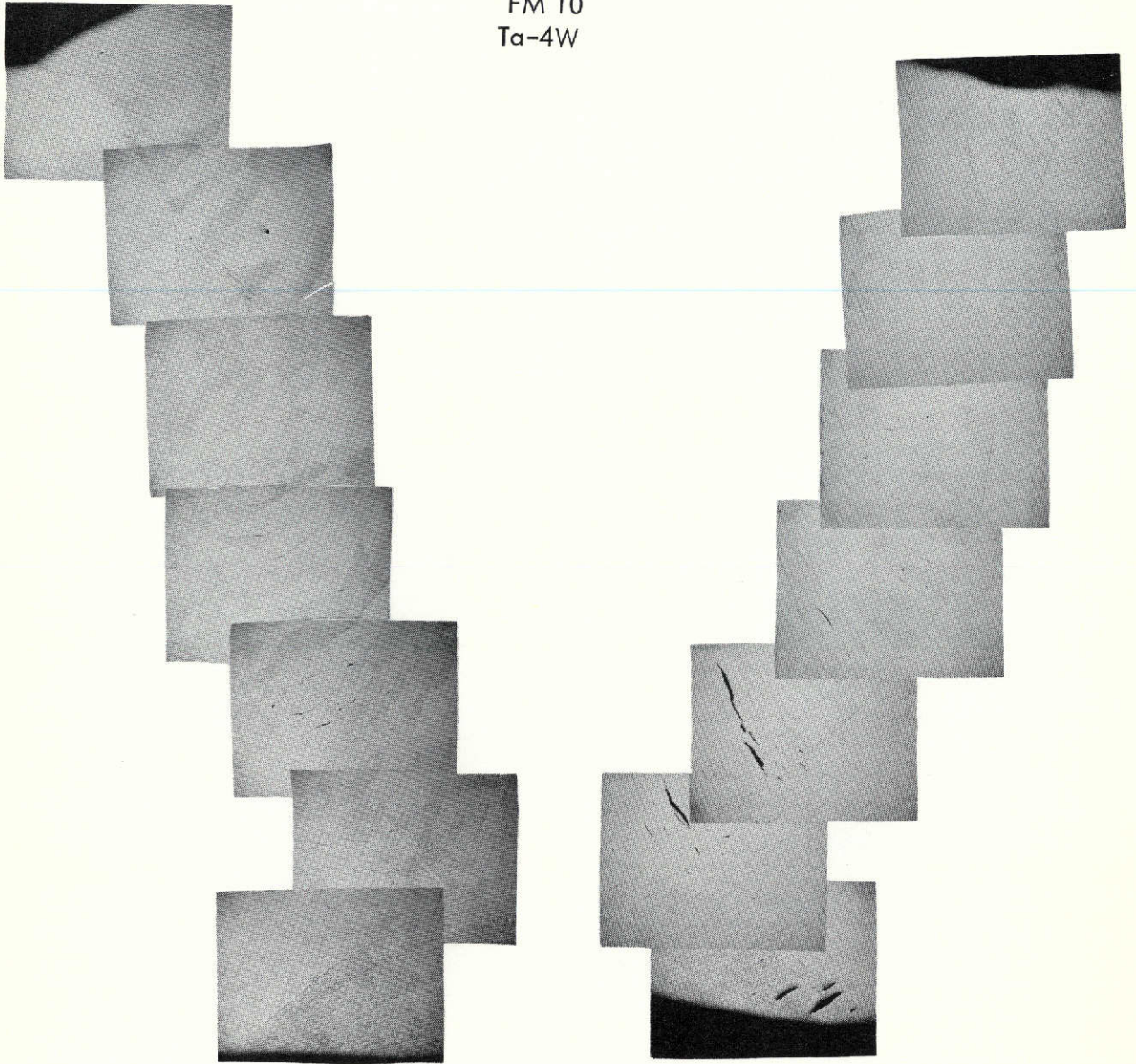
Weld 19
FM 4
Ta-4W-1Hf

AFTER

BEFORE

Figure 33. Microstructure of Single "V" Weld 19 - Before and After Bend Testing

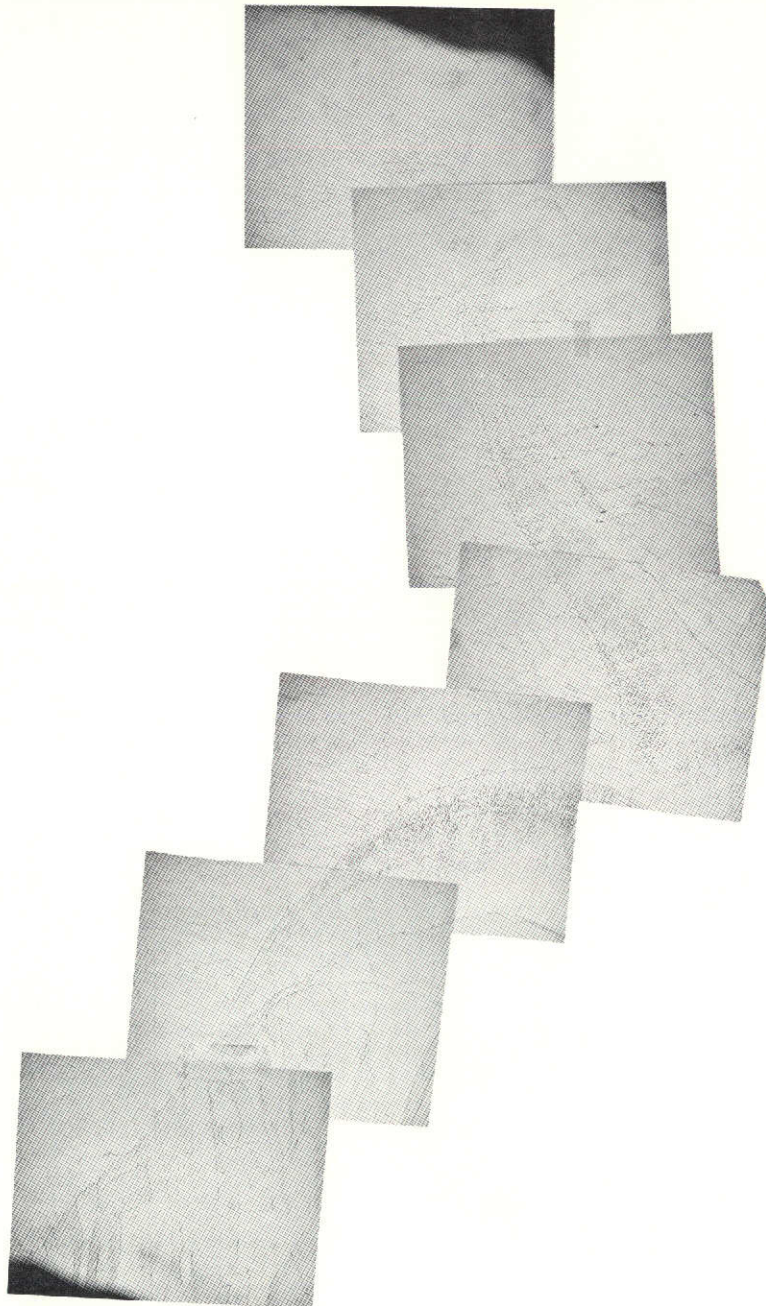
Weld 24
FM 10
Ta-4W



BEFORE

AFTER

Figure 34. Microstructure of Single "U" Weld 24 - Before and After Bend Testing



Weld 23
FM 10
Ta-4W

Tension
←————→

Figure 35. Typical Microstructure of Double "V" Weld 23 Following Bend Test at Room Temperature

metal were 2% and 1%, respectively. Counts were recorded and compared with the background. Although the exact hafnium content was not determined, relative measurements indicated:

- In the T-111 base metal, hafnium concentrations vary little with location.
- Hafnium in the weld metal varied from that of the filler metal to that of T-111, being greatest adjacent to the grain boundaries.
- There is not an abrupt change in hafnium content in going from base metal to weld metal. The dilution of hafnium from the base metal, which occurs during welding, produces a quasi-uniform concentration gradient within the weldments.

4.8 HARDNESS TESTS

Hardness traverses were made on representative specimens taken from welds 2, 4, 6, 8, 18, and 21 to measure property variations within the weld. The results are shown in Table 12. The location of each hardness reading is shown in Figure 36. In general, the hardness results indicate that a significant amount of filler metal-base metal mixing occurs in most of the weld zone and is not confined to the weld metal-HAZ interface. These results substantiate the variations in hafnium content previously reported. The hardness in the top bead is most representative of the undiluted filler metal hardness. For weld 2, the filler metal, FM 3 (Ta-6W-1.5Hf), had about the same hardness as the base metal; thus, there is very little hardness variation within the weld. Welds 4, 6, and 18 have filler metals significantly softer than the base metal, and large variations in hardnesses were observed. The hardnesses at the roots of these welds were the highest within the weld metal because of the greater mixing in this area. The hardness of FM 8 used in weld 8 is greater than the base metal; thus, the root area is the lowest hardness within the weld. Similar correlation between filler metal-base metal mixing was observed in the results of the hardness traverse

Table 12. Weldment Hardness Results

Weld No. FM Joint	2 3 Single "V"	4 4 Single "V"	6 5 Single "V"	8 8 Single "V"	18 10 Single "V"	21 4 Double "V"
A	206	173	183	289	127	191
B	202	179	183	292	131	212
C	197	173	183	294	127	218
D	189	170	193	279	136	219
E	193	175	181	279	133	218
F	212	172	187	276	129	-
G	201	193	199	276	166	227
H	210	205	203	258	167	210
I	212	201	213	262	168	209
J	218	-	222	235	175	203
K	213	216	224	224	166	191
L	199	207	205	209	206	212
M	205	202	205	218	207	-
N	209	190	191	241	134	-

(Values are in DPH units.)

Also, see Figure 36.

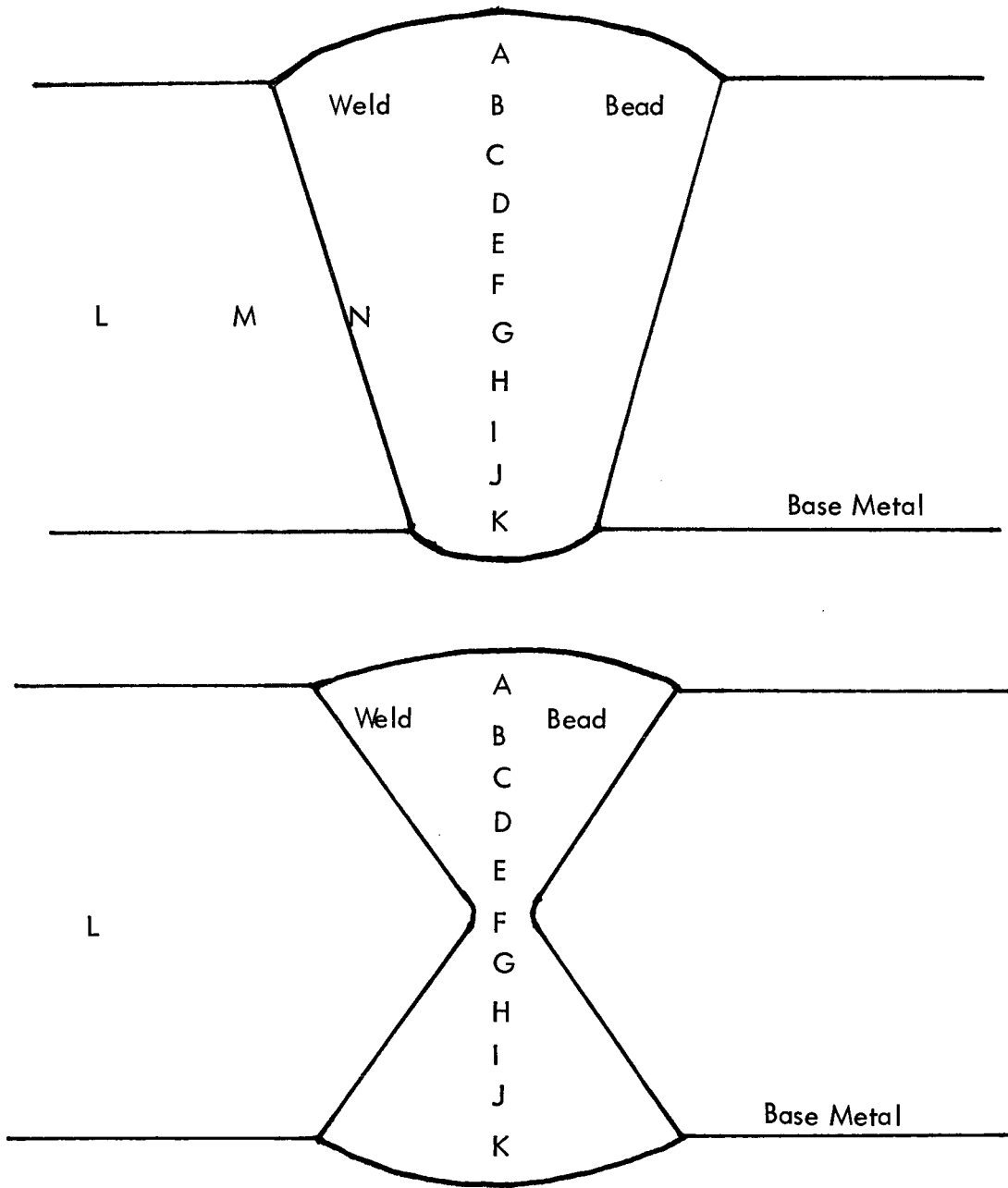


Figure 36. Schematic: Location of Hardness Measurements on Plate Weldments. Data Tabulated on Table 12.

taken on weld 21, FM 4, which was of the double "V" geometry. The minimum hardness observed in this weld was 191 DPH and compares to a minimum hardness of 170 DPH observed in weld 4, FM 4. The filler metals are of the same composition, only the weld geometry differed. The double "V" is a "tighter" joint than the single "V" is and subject to greater filler metal-weld metal mixing; hence, the resulting weld has a hardness nearer that of the base metal.

The observed hardness difference between the double and single "V" joints agrees with the previously measured and discussed differences in mechanical strength between the two joints; i. e., the specimens taken from the double "V" joint are stronger than those taken from a single "V" joint, all other parameters being equal.

5.0 CONCLUSIONS

This program was directed to reducing or eliminating underbead cracking in T-111 GTA multipass plate welds. The following are the major conclusions reached regarding welding of T-111 plate.

1. Multipass (greater than 6 passes) single "V" GTA welds in thick T-111 plate result in underbead cracking regardless of the filler metal used. The presence of hafnium in the weld metal inherently results in grain boundary cracking if substantial weld deformation occurs, as in the single "V" joint.
2. Using two fill passes and filler metals containing no hafnium, crack-free welds can be successfully accomplished with the single "V" joint.
3. Crack-free welds can be made in double "V" joints with hafnium-containing filler metals.
4. Of all the hafnium containing filler metals tested, FM 4 (Ta-4W-1Hf) was the best based upon the reduction of underbead cracking propensity.
5. Results of the screening of filler metals performed with the Varestraint test correlated well with the observed butt welding behavior.
6. The reduction in matrix to grain boundary strengths is not a directly viable solution to the problem of underbead cracking in T-111 plate. To eliminate or reduce underbead cracking, the imposed stress-strain state along with the hafnium content at the weld metal grain boundaries must be minimized.

6.0 REFERENCES

1. Gold, R. E. and Lessmann, G. G., "Influence of Restraint and Thermal Exposure on Welds in T-111 and ASTAR-811C", NASA CR-72858, January 1971.
2. Ekvall, R. A., Frank, R. G., and Young, W. R., "T-111 Alloy Cracking Problems During Processing and Fabrication", paper in NASA SP-245, June 1969.
3. Stoner, D. R. and Buckman, R. W. Jr., "Development of Large Diameter T-111 Tubing", NASA CR-72869, April 1971.
4. Lessmann, G. G. and Gold, R. E., "Long-Time Elevated Temperature Stability of Refractory Metal Alloys", Part II of "Determination of Weldability and Elevated Temperature Stability of Refractory Metal Alloys", NASA CR-1608, September 1970.
5. Lessmann, G. G. and Gold, R. E., "The Vareststraint Test for Refractory Metals", NASA CR-72828, November 1970.
6. Savage, W. F. and Lundin, C. D., "The Vareststraint Test", *Welding Journal, Research Supplement*, 44 (10), pp. 433-s to 442-s, (1965).
7. Buckman, R. W. Jr. and Goodspeed, R. C., "Development of Precipitation Strengthened Tantalum Base Alloys", NASA CR-1642, May 1971.

DISTRIBUTION LIST

NASA-Lewis Research Center
Attn: P. E. Moorhead, MS 106-1
R. L. Davies, MS 106-1
N. T. Saunders, MS 105-1
R. E. Gluyas, MS 105-1
R. W. Hall, MS 105-1
W. D. Klopp, MS 105-1
R. E. English, MS 500-201
R. Brietweiser, MS 302-1
E. J. Kolman, MS 500-313
Tech. Util. Ofc., MS 3-19
T. J. Moore, MS 105-1 (3)
21000 Brookpark Road
Cleveland, OH 44135

NASA Headquarters
Attn: Library
Washington, DC 20546

NASA Headquarters
Attn: RW/G. Deutsch
RWM/J. Gangler
Washington, DC 20546

NASA-Ames Research Center
Attn: Library
Moffett Field, CA 94035

NASA-Jet Propulsion Laboratory
Attn: Library
J. Mondt, 122-123
W. Phillips
4800 Oak Grove Drive
Pasadena, CA 91103

NASA-Langley Research Center
Attn: Library
W. Brooks
B. Stein
Hampton, VA 23365

NASA-Johnson Spacecraft Center
Attn: Library
R. Johnson
Houston, TX 77058

NASA-George C. Marshall Space
Flight Center
Attn: Library
C. Riehl
C. McKannon
C. Cataldo
Marshall Space Flight Center, AL
53812

NASA-Scientific and Technical
Information Facility
Attn: NASA Representative
P. O. Box 5700
Bethesda, MD 20014

AiResearch Manufacturing Company
Attn: Library
Sky Harbor Airport
402 South 36th Street
Phoenix, AZ 85041

AiResearch Manufacturing Company
Attn: Library
9851-9951 Sepulveda Blvd.
Los Angeles, CA 90045

Argonne National Laboratory
Attn: Library
9700 South Gross Avenue
Argonne, IL 60439

Army Ordnance Frankford Arsenal
Attn: Library
Bridesburg Station
Philadelphia, PA 19137

Atomics International
Attn: Library
T. Moss
W. Botts
H. Pearlman
8900 DeSoto Avenue
Canoga Park, CA 91303

Bureau of Ships
 Department of the Navy
 Attn: Library
 Washington, DC 20390

Battelle Memorial Institute
 Attn: Library
 D. L. Keller
 P. Gripshover
 B. Wilcox
 Columbus Laboratories
 Columbus, OH 43201

Battelle Memorial Institute
 Attn: Library
 Pacific Northwest Laboratories
 Richland, WA 99352

Boeing Aircraft Corporation
 Attn: Library
 Seattle, WA 98124

Bureau of Weapons
 Research and Engineering
 Material Division
 Attn: Library
 Washington, DC 20390

Brookhaven National Laboratory
 Attn: Library
 Upton, Long Island, NY 11973

Chance Vought Aircraft, Inc.
 Attn: Library
 P. O. Box 4907
 Dallas, TX 75222

Clevite Corporation
 Mechanical Research Division
 Attn: Library
 540 East 105th Street
 Cleveland, OH 44108

Climax Molybdenum Company of
 Michigan
 Attn: Library
 Detroit, MI 48202

Convair Astronautics
 Attn: Library
 5001 Kearny Villa Road
 San Diego, CA 92111

Electro-Optical Systems, Inc.
 Advanced Power Systems Division
 Attn: Library
 Pasadena, CA 91105

Fansteel Metallurgical Corporation
 Attn: Library
 A. Dana
 North Chicago, IL 60064

Ford Motor Company
 Aeronutronics
 Attn: Library
 Newport Beach, CA 92660

General Electric Company
 Vallecitos Atomic Laboratory
 Attn: Library
 Pleasanton, CA 94566

United Nuclear Corporation
 Attn: Library
 5 New Street
 White Plains, NY 10601

University of Michigan
 Department of Chemical and
 Metallurgical Engineering
 Attn: Library
 Ann Arbor, MI 48105

U. S. Atomic Energy Commission
 Attn: Tech. Reports Library
 J. Simmons
 C. Tarr
 N. Goldenberg
 Washington, DC 20525

U. S. Atomic Energy Commission
 Technical Information Service Ext.
 P. O. Box 62
 Oak Ridge, TN 37831 (3 copies)

U. S. Naval Research Laboratory
Attn: Library
Washington, DC 20390

Vought Astronautics
Attn: Library
P. O. Box 5907
Dallas, TX 75222

Wah Chang Corporation
Attn: Library
S. Worcester
Albany, OR 97321

Westinghouse Electric Corporation
Aerospace Electric Division
P. O. Box 989
Lima, OH 45802

Westinghouse Electric Corporation
Astronuclear Laboratories
Attn: Library
R. Buckman (2 copies)
P. O. Box 10864
Pittsburgh, PA 15236

Westinghouse Electric Corporation
Research Laboratories
Attn: Library
R. T. Begley
Churchill Borough, PA 15235

Wolverine Tube Division
Calumet and Hecla, Inc.
Attn: Librarian
2525 Beech-Daly Road
Dearborn Heights, MI 48125

Wright-Patterson Air Force Base
Air Force Materials Laboratory
Attn: N. Geyer
T. Cooper
Library
J. L. Morris
H. J. Middencorp, ASNRC
33143
C. L. Harmsworth
Dayton, OH 45433

Wyman-Gordon Company
Attn: Library
North Grafton, MA 01536

General Atomic
John Jay Hopkins Laboratory
Attn: Library
L. Yang
W. Holland
P. O. Box 608
San Diego, CA 92112

General Dynamics
Attn: Library
P. O. Box 748
Fort Worth, TX 86101

General Electric Company
Atomic Power Equipment Division
Attn: Library
P. O. Box 1131
San Jose, CA 95108

General Electric Company
Aircraft Engine Group
Attn: W. H. Chang, M78
FPD Tech. Info. Center, F-22
Evendale, OH 45215

General Electric Company
Missile & Space Vehicle Department
Attn: Library
3198 Chestnut Street
Philadelphia, PA 19104

General Motors Corporation
Allison Division
Attn: Library
Indianapolis, IN 46206

Grumman Aircraft Company
Attn: Library
Bethpage, Long Island, NY 11100

Hamilton Standard
Division of United Aircraft Corp.
Attn: Library
Windsor Locks, CT 06096

Hughes Aircraft Company
Engineering Division
Attn: Library
Culver City, CA 90230

Johns Hopkins University
Applied Physics Laboratory
Attn: Library
8621 Georgia Avenue
Silver Spring, MD 20910

Franklin Institute
Attn: Library
A. Lawley
Philadelphia, PA 19103

Lawrence Radiation Laboratory
Technical Information Division
Attn: Library
W. Myers
Livermore, CA 94550

Lockheed Missiles and Space Division
Lockheed Aircraft Corporation
Attn: Library
R. A. Perkins
Sunnyvale, CA 94086

Los Alamos Scientific Laboratory
Attn: Library
J. Taub
Los Alamos, NM 87544

Manlabs, Inc.
Materials Research and Development
Attn: Library
21 Erie Street
Cambridge, MA 02139

Marquardt Aircraft Company
Attn: Library
P. O. Box 2013
Van Nuys, CA 91404

McDonnell-Douglas Astronautics Co., West
Attn: Library
Santa Monica, CA 90406

Temescal Metallurgical
Attn: Library
2850 7th Street
Berkeley, CA 94710

Thermo Electron Engineering Corp.
Attn: Library
G. Hatsopoulos
85 First Avenue
Waltham, MA 02154

TRW Systems
Attn: Mathew King
Nuclear Technology Dept.
D. Carrol
Library
One Space Park
Redondo Beach, CA 90278

TRW Equipment Laboratories
Attn: Library
23555 Euclid Avenue
Cleveland, OH 44117

Union Carbide Corporation
Parma Research Center
Technical Information Service
Attn: Library
P. O. Box 6116
Cleveland, OH 44101

Union Carbide Metals
Attn: Library
Royal Avenue
Niagara Falls, NY 14303

H. Nagler
Code A934
Naval Ship Research and Development
Laboratory
Annapolis, MD 21402

Donald J. Sandstrom
CMB-6 Fabrication Section
Los Alamos Scientific Laboratory
P. O. Box 1663
Los Alamos, NM 87544

M. M. Schwartz, Manager
 Manufacturing Research and Technology
 Department
 405 Rohr Corporation
 P. O. Box 878, Mail Zone 29T
 Chula Vista, CA 92012

J. Vagi
 Advanced Technology Department
 Naval Nuclear Fuels Division
 Babcock and Wilcox Company
 P. O. Box 785
 Lynchburg, VA 24505

Terrence R. Webster
 Teledyne Wah Chang
 P. O. Box 460
 Albany, OR 97321

R. H. Witt, Group Leader
 Advanced Materials and Process
 Development
 Plant XII, Department 447
 Grumman Aerospace Corporation
 Bethpage, NY 11714

S. A. Worcester
 Technical Division
 Teledyne-Wah Chang Albany
 P. O. Box 460
 Albany, OR 97321

K. C. Wu
 Northrop Corporation
 Aircraft Division
 Orgn. 3771/Zone 62
 3901 West Broadway
 Hawthorne, CA 90250

G. M. Slaughter
 Metals and Ceramics Division
 Oak Ridge National Laboratory
 Union Carbide Corporation
 Nuclear Division
 P. O. Box X
 Oak Ridge, TN 37830

S. D. Barth, Welding Engineer
 Nooter Corporation
 1400 S. 3rd Street
 St. Louis, MO 63166

Alexander Bosna
 General Electric Company
 Reentry and Environmental Division
 P. O. Box 8555
 Philadelphia, PA 19101

J. R. Condra
 E. I. DuPont de Nemours Company
 Chambers Works
 Deepwater, NJ 08023

James R. Doyle
 Pratt & Whitney Aircraft
 MDL-J Building Mezanine
 400 Main Street
 East Hartford, CT 06018

Thomas J. Enright
 Eastern Laboratory
 E. I. duPont Company
 Gibbstown, NJ 08027

E. A. Franco-Ferreira
 Tennessee Forging Steel Company
 Harriman, TN 37748

J. M. Gerken
 T/M 3039, Materials Technology
 TRW, Inc.
 23555 Euclid Avenue
 Cleveland, OH 44117

S. Goldstein
 Kawecki-Beryllium Corporation
 P. O. Box 1462
 Reading, PA 19603

J. M. Gray
 Molybdenum Corporation of America
 Room 1312
 4 Gateway Center
 Pittsburgh, PA 15317

M. A. Greenfield
Joining Technology Section
Metals Branch
Air Force Materials Laboratory
Wright-Patterson Air Force Base, OH
45433

W. Hatch
Army Materials and Mechanics
Research Center
Watertown, MA 02172

David C. Hill
Union Carbide Corporation
Tarrytown Technical Center
Old Saw Mill River Road
Tarrytown, NY 10591

K. H. Koopman
Welding Research Council
345 E. 47th Street
New York, NY 10017

G. G. Lessmann
Westinghouse Electric Corporation
Research and Development Center
Pittsburgh, PA 15235

A. J. Moorhead
Metals and Ceramics Division
Oak Ridge National Laboratory
Oak Ridge, TN 37830

Morris W. Mote
Sandia Corporation
Livermore Laboratory
P. O. Box 969
Livermore, CA 91550